bioRxiv preprint doi: https://doi.org/10.1101/2020.08.24.264689; this version posted August 24, 2020. The copyright holder for this preprint (which was not certified by peer review) is the author/funder, who has granted bioRxiv a license to display the preprint in perpetuity. It is made available under aCC-BY 4.0 International license.

An essential amino acid synchronises malaria parasite development with daily host rhythms

Kimberley F. Prior[1,2], Benita Middleton[3], Alíz T.Y. Owolabi[1,2], Mary L. Westwood[1,2], Jacob Holland[1,2], Aidan J. O'Donnell[1,2], Mike Blackman[4,5], Debra J. Skene[3], Sarah E. Reece[1,2]

Institutes of Evolutionary Biology[1] and Immunity & Infection Research[2], University of Edinburgh, UK; Faculty of Health and Medical Sciences, University of Surrey[3], UK; Malaria Biochemistry Laboratory[4], The Francis Crick Institute, UK; Faculty of Infectious and Tropical Diseases[5], London School of Hygiene & Tropical Medicine, UK.

Summary

The replication of blood-stage malaria parasites is synchronised to the host's daily feeding rhythm. We demonstrate that a metabolite provided to the parasite from the host's food can set the schedule for *Plasmodium chabaudi's* intraerythrocytic development cycle (IDC). First, a large-scale screen reveals multiple rhythmic metabolites in the blood that match the timing of the IDC, but only one - the amino acid isoleucine - that malaria parasites must scavenge from host food. Second, perturbing the timing of isoleucine provision and withdrawal demonstrate that parasites use isoleucine to schedule and synchronise their replication. Thus, periodicity in the concentration of isoleucine in the blood, driven by host-feeding rhythms, explains why timing is beneficial to the parasite and how it coordinates with host rhythms. Blood-stage replication of malaria parasites is responsible for the severity of disease symptoms and fuels transmission; disrupting metabolite-sensing by parasites offers a novel intervention to reduce parasite fitness.

Keywords

Plasmodium, periodicity, synchrony, circadian rhythm, feeding time, metabolism, metabolomics, intraerythrocytic development cycle, isoleucine, asexual replication

bioRxiv preprint doi: https://doi.org/10.1101/2020.08.24.264689; this version posted August 24, 2020. The copyright holder for this preprint (which was not certified by peer review) is the author/funder, who has granted bioRxiv a license to display the preprint in perpetuity. It is made available under aCC-BY 4.0 International license.

Introduction

Causing over 200 million cases and 400,000 deaths per year, malaria remains notorious as a major infectious disease (World Malaria Report 2019). The timing and synchrony exhibited by malaria parasites (*Plasmodium*) during successive cycles of blood-stage replication underpins the parasite's abilities to establish and maintain an infection, and to transmit to mosquitoes (Prior et al 2020). The intraerythrocytic development cycle (IDC) is characterised by parasite invasion and subsequent growth and division within the red blood cells (RBCs), followed by bursting to release the next cohort of asexually replicating parasites. How and why the vast majority of *Plasmodium* species progress though the different development stages of the IDC in synchrony with each other, and why transitions between these stages occur at particular times of day, are long standing mysteries (Hawking 1970, Garcia et al 2001, Reece et al 2018). Given that asexual replication is responsible for the disease symptoms of malaria and fuels the production of transmission forms, understanding how the IDC is scheduled (i.e. the developmental synchrony between parasites and the timing of IDC stage transitions, Mideo et al 2013) may unlock novel interventions or improve the efficacy of existing treatments.

Parasites have an intrinsic time-keeping mechanism which they use to maintain synchrony with the host's daily rhythms (Rijo-Ferreira et al 2020, Smith et al 2020, Subhudhi et al 2020). However, the identity of the host rhythm(s) that parasites align to and why this matters for their fitness remain unknown (O'Donnell et al 2011, Prior et al 2020). The IDC schedule is aligned to host daily rhythms driven by feeding rhythms (Hirako et al 2018, Prior et al 2018), but not the act of eating itself (Rijo-Ferreira et al 2020), and the relevant host rhythm occurs independently of processes directly controlled by host circadian clocks (O'Donnell et al 2019). These findings suggest rhythmicity in the concentration of a resource (e.g. nutrient, metabolite, growth factor) that appears in the blood as a consequence of food digestion provides the cue for timing the IDC schedule (Prior et al 2020). Glucose has been proposed as such a driver (Hirako et al 2018, Prior et al 2018): during the host's resting phase (i.e. daytime for mice) blood glucose concentration is at its nadir and the IDC is characterised by the low-energy consuming "ring stage". During the host's active phase, host feeding elevates blood glucose and parasites transition into the high-energy consuming late trophozoite stage before maturing as schizonts and become ready to burst (Olszewski and Llinás 2011).

Beyond glucose, IDC completion is sensitive to several other aspects of the within-host environment. For example, both isoleucine starvation (Babbitt et al 2012) and antimalarial drug treatment (Codd et al 2011) can induce both delayed development and dormancy. The parasite's resource requirements vary throughout the IDC with, for example, demands on glycerophospholipids and amino acids to fuel biogenesis, increasing after the transition to trophozoites (Olszewski et al 2009, Déchamps et al 2010). Parasites can biosynthesise some metabolites themselves (for example, glutamic acid from carbon dioxide fixation), others are taken up from the RBCs or blood plasma (for example, glucose), whereas most amino acids are acquired from haemoglobin digestion (Sherman 1979). Whether all the resources that all the parasites within an infection need are available around-the-clock or are limited to a certain time of day (due to host daily rhythms and/or the parasite's ability to acquire them) is unknown.

We take an evolutionary ecology and chronobiology approach to investigate whether the concentration of an essential resource(s) in the blood, arising from host feeding-driven rhythms, sets the timing of the IDC schedule. Under this hypothesis, parasites developing too fast or too slow will be at the wrong IDC stage when the resource(s) is available, and suffer when they transition to the IDC stage most in need of the resource. This blood-borne scheduling force could set the timing of the IDC via two mechanisms. These mechanisms are not mutually exclusive and, in the case of an essential resource that is only available during a certain window each day, likely operate in concert. First, a mismatch between IDC stage and resource supply causes starvation, leading to a high death rate of parasites not "on time". Second, parasites actively shift their IDC schedule if they detect a mismatch between IDC stage and resource supply, with their response avoiding starvation. In support of the second scenario, parasites can modulate their developmental rate via serpentine receptor 10 (Subudhi et al 2020), and enter a period of dormancy in response to loss of some nutrients (as observed for *P. falciparum* in response to isoleucine withdrawal; Babbitt et al 2012, McLean and Jacobs-Lorena 2020).

Here, we capitalise on the rodent malaria *P. chabaudi* model system in which *in vivo* experiments exploit ecologically relevant host-parasite interactions and short-term *in vitro* studies allow within-host ecology to be probed in-depth (Grech et al 2006, Spence et al 2011). First, we conduct a hypothesis-driven screen of several metabolite classes to identify those with daily fluctuations in the blood and whose rhythm coincides with the time-of-day that hosts feed and with the IDC schedule (Skene et al 2018). This experiment revealed only one candidate that happens to be both essential to the parasite and provided solely from the host's food: isoleucine. Second, we withdraw isoleucine from parasites *in vitro* for different durations and quantify the effects on IDC progression. We find that development stalls upon isoleucine removal, but restarts and continues at the same rate regardless of how

bioRxiv preprint doi: https://doi.org/10.1101/2020.08.24.264689; this version posted August 24, 2020. The copyright holder for this preprint (which was not certified by peer review) is the author/funder, who has granted bioRxiv a license to display the preprint in perpetuity. It is made available under aCC-BY 4.0 International license.

long isoleucine is absent, and that isoleucine removal does not elevate parasite mortality in these conditions. Our findings are consistent with parasites using isoleucine as a time-of-day cue, and with the concept that parasite control of the IDC schedule protects them from starvation and facilitates maximal exploitation of host resources.

Results

Metabolites that associate with host feeding/fasting rhythms and the IDC

To identify metabolites whose rhythms correspond to the timing of host feeding and the IDC schedule, we compared four groups of malaria infections in mice that were either wild type (WT) C57BL/6J strain or *Per1/2*-null circadian clock-disrupted mice (previously backcrossed onto a C57BL/6J background for 10 generations). *Per1/2*-null mice have an impaired TTFL clock (Transcription Translation Feedback Loop, which forms the molecular basis of the classical circadian clock) and exhibit no TTFL-driven circadian rhythms in physiology or behaviour when kept in constant darkness (Bae et al 2001, Maywood et al 2014). We generated 3 different groups of hosts whose feeding rhythms differed with respect to the light:dark cycle and whether they had an intact TTFL clock, and a 4th group of hosts which lacked both feeding rhythms and an intact TTFL clock (Fig 1A). Parasites exhibit high amplitude IDC rhythms in the 3 groups of mice with feeding rhythms (the phase of the IDC coinciding with the phase of host feeding), and parasites in the 4th group show severely dampened rhythms (Fig 2; O'Donnell et al 2019). To explain how the parasite IDC is linked to host rhythms, a time-cue/time-dependent resource must vary or have rhythmicity across the day, with a peak concentration that associates with the timing of host feeding as well as the same parasite IDC stage, across all 3 treatment groups with rhythmic feeding and a rhythmic IDC, yet be arrhythmic in the 4th group (Fig 1B). Thus, we identified candidate metabolites by intersecting rhythmic metabolites in each of our treatment groups. Specifically, having verified that the IDC schedules followed the expected patterns across the treatment groups (Fig 2, Supp Table 1) we intersected metabolites rhythmic in dark (i.e. night) feeding (DF, n=18) and light (i.e. day) feeding (LF, n=17) WT mice: in DF and LF mice parasites have inverted IDC timing but host TTFL clocks are intact, and so any rhythmic metabolites in the blood could arise directly from via TTFL clock-driven processes or via TTFL clock-independent food-processing rhythms (Fig 1B). Next, we intersected those metabolites rhythmic in DF and LF WT mice with rhythmic metabolites in *Per1/2*-null mice (whose metabolites appear in the blood from TTFL clock independent processing of food (O'Donnell et al 2019)) that feed during a time-restricted 12 h window in constant darkness (TRF mice, n=17; Fig 1B). Finally, we removed metabolites from the intersected list that remained rhythmic in *Per1/2*-null mice with no feeding rhythm or TTFL clock (ALF mice, n=16) because parasites in these hosts exhibit dampened rhythms (O'Donnell et al 2019). We then determined the phase of each candidate metabolite (using peak time-of-day as a phase marker) in the intersection between the 3 groups with feeding rhythms and tested for an association with the timing (phase) of the parasite IDC.

bioRxiv preprint doi: https://doi.org/10.1101/2020.08.24.264689; this version posted August 24, 2020. The copyright holder for this preprint (which was not certified by peer review) is the author/funder, who has granted bioRxiv a license to display the preprint in perpetuity. It is made available under aCC-BY 4.0 International license.

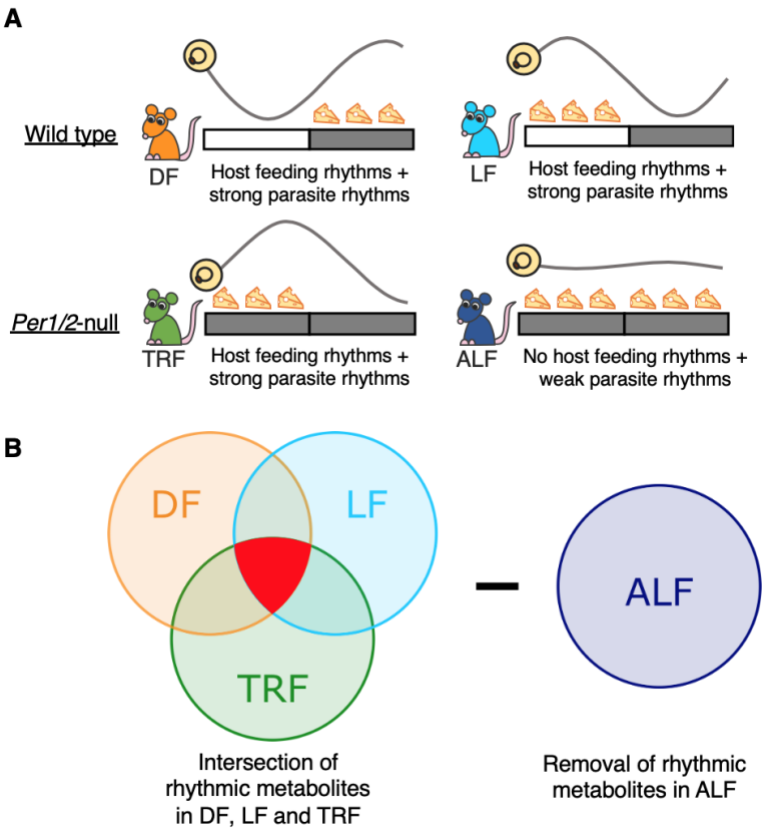

Fig 1. Experimental design. A) Wild type mice were housed in the same 12h light: 12h dark regime (indicated by the light-dark bar) and were given unrestricted access to food for 12 hours either during the night-times (DF, dark feeding) or the day times (LF, light feeding) as indicated by the position of the cheeses. Per1/2-null mice were housed in continuous darkness (DD) and either experienced cycles of 12-hours followed by 12 h without access to food (TRF, time restricted feeding,) or given constant access to food (ALF, ad-libitum feeding). DF, LF and TRF mice have feeding rhythms and the parasite IDC is rhythmic. ALF mice do not have a feeding rhythm (O'Donnell et al 2019), and so, the IDC rhythm is substantially dampened. B) Metabolites that were significantly rhythmic in DF, LF and TRF mice (highlighted in red), but not in ALF mice, were considered further. Treatment groups colour coded: DF=orange, LF=light blue, TRF=green, ALF=dark blue.

bioRxiv preprint doi: https://doi.org/10.1101/2020.08.24.264689; this version posted August 24, 2020. The copyright holder for this preprint (which was not certified by peer review) is the author/funder, who has granted bioRxiv a license to display the preprint in perpetuity. It is made available under aCC-BY 4.0 International license.

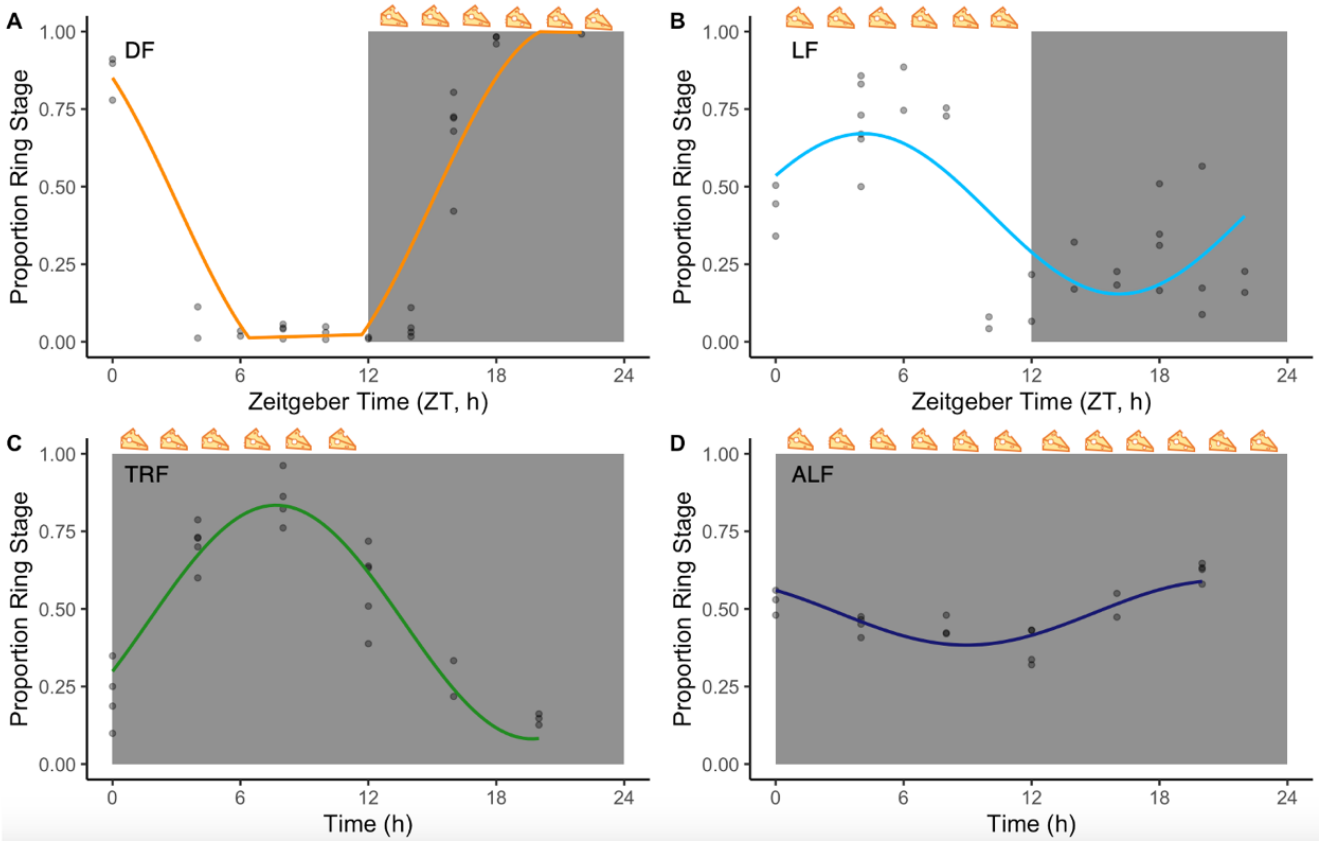

Fig 2. IDC schedule (determined by the proportion of parasites at ring stage) coincides, as expected, with feeding rhythms. A) DF: dark feeding WT mice food access ZT 12-24 (12 h at night) in 12h:12h light:dark, B) LF: light feeding WT mice food access ZT 0-12 (12 h in day) in 12 h:12 h light:dark, C) TRF: time restricted feeding Per1/2-null mice food access 0-12 hours (12 h at the same time (GMT) as LF mice) in constant darkness (DD), D) ALF: ad libitum feeding Per1/2-null mice access in constant darkness (see Fig 1 for Experimental Design and more details). The white panel denotes lights on (Zeitgeber Time=0-12 h), dark grey panel denotes lights off (Zeitgeber Time=12-24 h for DF and LF, 0-24 h for TRF and ALF). The cheeses along the top of the plots denotes the feeding window. The line is the model fit for each group and the black dots are the raw data (n= 2-5 infections per time point – the thin blood smears from several mice were of insufficient quality, explaining the uneven number of data points). The fitted sine/cosine curve for DF (A) is distorted due to a large amplitude which exceeds the bounds possible for proportion data (between 0 and 1) so is truncated for visualisation. Parasite rhythms follow the time of host food intake. All groups are explained better by sine/cosine curves than by a straight line (see Supp Table 1), however there are differences in amplitude and thus degree of "rhythmicity". Specifically, the lowest amplitude of ring stages across the day is found in the ALF group and the highest in the DF group (defined as the difference between maximum and minimum proportion of ring stages across the day: DF=1, LF=0.52, TRF=0.73, ALF=0.21). The peak timing also differs between groups according to feeding, peaking 0-12 h for LF and TRF groups and 12-24 h for the DF group (DF=ZT 21, LF=ZT 4.1, TRF=7.3 hours). Parasites in ALF mice have a minor peak at 21.2 hours due to low amplitude rhythms.

We sampled mice every 2 hours from day 5 post infection (when infections are at a low parasitaemia, ~10%, to minimise the contribution of parasite molecules to the dataset) for 26 hours and 10 µl blood plasma was collected from each mouse for targeted LC/MS metabolomics to quantify 134 different metabolites spanning 6 different metabolite classes (Supp Table 2). Blood glucose concentration was measured using a glucometer, and thin blood smears were made to verify that IDC rhythms were as expected: rhythmic in DF, LF and TRF, with opposite phase in DF versus LF/TRF, and dampened rhythms in ALF (Fig 2, Supp Table 1; O'Donnell et al 2019). We defined daily rhythmicity in the concentrations of the 134 metabolites detected by the UPLC/MS-MS platform as the detection of rhythmicity in at least 2 of the following circadian analysis programmes: ECHO (https://github.com/delosh653/ECHO), CircWave (https://www.euclock.org/results/item/circ-wave.html) and JTK_Cycle (https://openwetware.org/wiki/HughesLab:JTK_Cycle). For metabolites not found to be rhythmic by at least 2 of the circadian analysis programmes, we also carried out Analysis of Variance to identify metabolites that varied across the day but without a detectable 24 h rhythm (Supp Table 3 for breakdown of which candidate metabolites were rhythmic in each programme).

bioRxiv preprint doi: https://doi.org/10.1101/2020.08.24.264689; this version posted August 24, 2020. The copyright holder for this preprint (which was not certified by peer review) is the author/funder, who has granted bioRxiv a license to display the preprint in perpetuity. It is made available under aCC-BY 4.0 International license.

Across the entire data set, 110 metabolites varied during the 26 h sampling window (101 in DF, 91 in LF, 50 in TRF and 1 in ALF; Supp Table 4 for full list of metabolites). That only 1 metabolite (lysoPC a C20:3) exhibited a rhythm in ALF hosts demonstrates the roles that host TTFL clocks and timed feeding play in generating metabolite rhythms (Reinke and Asher 2019). Next, we identified which of the 109 metabolites (after excluding lysoPC a C20:3, due to it being rhythmic in ALF mice) exhibited time-of-day variation in all of the DF, LF and TRF treatments (the red area in Fig 1B). This resulted in a list of 42 metabolites, consisting of 3 acylcarnitines, 11 amino acids, 9 biogenic amines and 19 glycerophospholipids (Fig 3A). We narrowed this list further by comparing whether the peak timing of the patterns exhibited by each of these 42 metabolites corresponded to the timing of the host's feeding rhythm and the parasite's IDC (Prior et al 2018, Hirako et al 2018). Specifically, feeding and IDC rhythms shared very similar phases in the LF and TRF mice (ZT/h 0-12 for LF and TRF, Fig 2, Supp Table 1), which were inverted in DF mice. Thus, the 33 metabolites whose peaks cluster away from the grey shaded areas in Fig 3B display inverted timing in the LF/TRF compared to DF mice and were retained for further analysis.

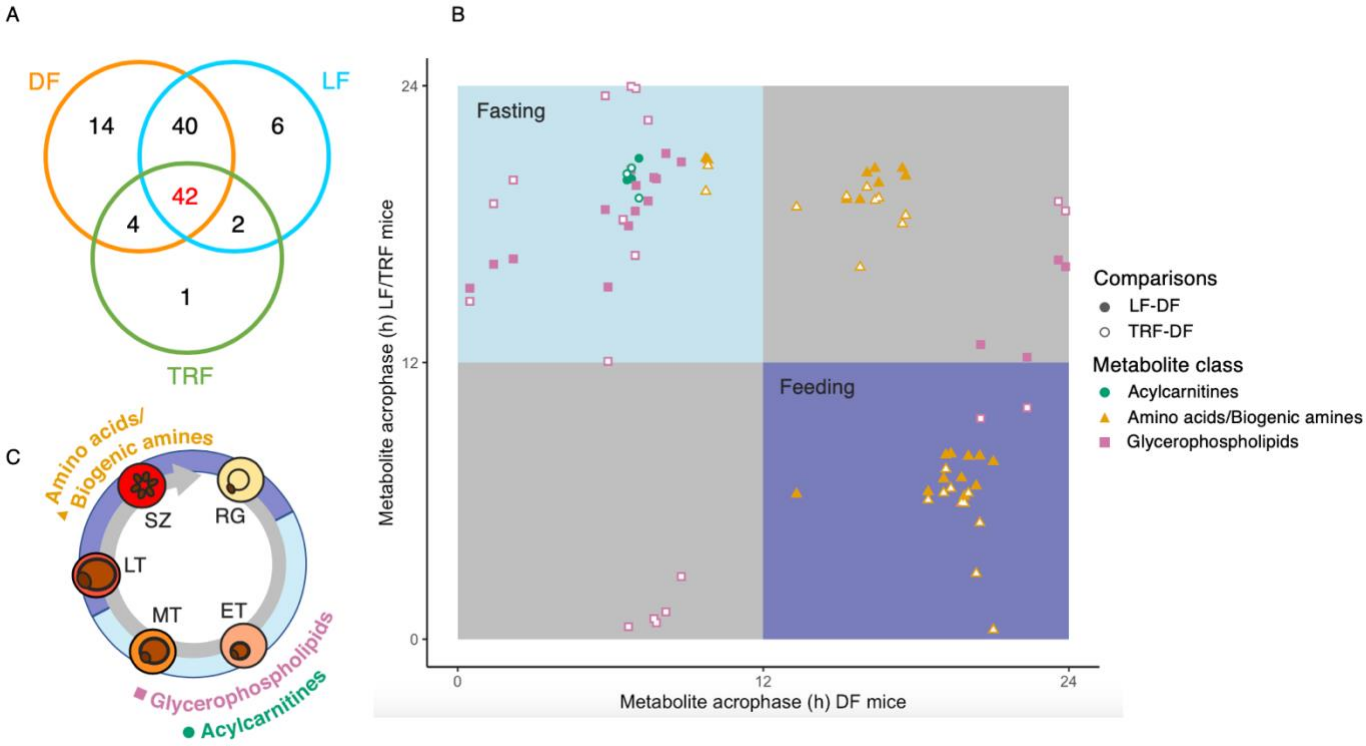

Fig 3. A) Venn diagram displaying the numbers of rhythmic intersecting metabolites out of a total of 109. B) The time of peak concentration of 42 candidate metabolites in the blood of DF, LF and TRF mice. Generally, metabolites in the top left panel (light blue) peak around the time hosts in all three groups are fasting while metabolites in the bottom right panel (dark blue) peak around the time hosts in all three groups are feeding, resulting in 33 candidates that are linked to the feeding-fasting cycle. TRF mice had the same feeding schedule as LF mice so the peak for each metabolite is plotted twice, for DF versus LF [closed points] and for DF versus TRF [open points] to reflect the opposing feeding and IDC rhythms in DF versus LF/TRF mice. Metabolite classes: acylcarnitines=green circles, amino acids/biogenic amines=orange triangles, glycerophospholipids=purple squares. See Supp Table 5 for peak times of each metabolite. C) Ring stages (RG), late trophozoites (LT) and schizonts (SZ) peak during the hosts feeding period (dark blue) which is generally when amino acids/biogenic amines peak in the blood. Early trophozoites (ET) and mid trophozoites (MT) peak during host fasting (light blue) when glycerophospholipids and acylcarnitines peak in the blood.

Linking metabolites to the IDC schedule

From the list of 33 metabolites whose peak associated with feeding and IDC timing, 13 amino acids and biogenic amines peaked during the feeding window (bottom right quadrant Fig 3B; 0-12 hours for LF and TRF, 12-24 hours for DF: corresponding to ZT0-12 for LF, ZT0-12h for TRF and ZT12-24 for DF). These metabolites are alanine, asparagine, isoleucine, leucine, methionine, phenylalanine, proline, threonine, valine, methionine-sulfoxide and serotonin. In contrast, 20 acylcarnitines and glycerophospholipids (with the exception of 2 biogenic amines) peaked

bioRxiv preprint doi: https://doi.org/10.1101/2020.08.24.264689; this version posted August 24, 2020. The copyright holder for this preprint (which was not certified by peer review) is the author/funder, who has granted bioRxiv a license to display the preprint in perpetuity. It is made available under aCC-BY 4.0 International license.

during the fasting window (top left quadrant Fig 3B; 12-24 hours for LF and TRF, 0-12 hours for DF: corresponding to ZT12-24 for LF, ZT0-12 for DF and 12-24 h for TRF). These metabolites are ADMA, SDMA, C14.1, C16, C18.1, lysoPCaC16:1, lysoPCaC18:1, lysoPCaC18:2, PCaaC32:1, PCaaC34:4, PCaaC38:3, PCaaC38:4, PCaaC38:5, PCaaC38:6, PCaaC40:4, PCaaC40:5, PCaeC34:3, PCaeC38:0, PCaeC38:3 and PCaeC42:1. See Supp Table 5 for peak times of each metabolite. During the fasting window, parasites are in the early IDC stages (rings, early-mid trophozoites), completing the IDC (late trophozoites-schizonts) halfway through the feeding window (Prior et al 2018 & Fig 3C). Each IDC stage has different requirements and fulfils different functions (Fig 4A). Could these candidate metabolites be involved in scheduling the parasite IDC, either by being sufficiently limiting at a certain time-of-day to enforce a rhythm on the IDC, and/or by acting as a time-of-day cue for a so-called "just-in-time" parasite strategy (or Zeitgeber if the parasite possesses a circadian clock) for the parasite to organise itself? Each of these scenarios require several non-mutually exclusive criteria to be met. First, for the IDC schedule to be enforced by rhythmicity in the availability of a metabolite, it requires that the parasite cannot overcome resource limitation by synthesising the metabolite itself. Second, if parasites use a resource as a time-of-day cue/Zeitgeber to schedule the IDC themselves, the peak timing of the metabolites related to the IDC schedule may coincide with the IDC stage(s) that most need them, or occur in advance and be perceived by an IDC stage before the one that needs it (i.e. analogous to anticipation). Third, for a metabolite to be a reliable time-of-day cue, it should be something the parasite cannot synthesise to prevent it having to differentiate between endogenous and exogenous information, and avoid the risk of mistakenly responding to an endogenous signal.

To what extent do the 33 acylcarnitines, glycerophospholipids and amino acids/amines candidates that associate with the feeding-fasting cycle meet these criteria? Acylcarnitines play a role in eukaryotic energy metabolism and mitochondria function by transporting fatty acids into the mitochondria. Glycerophospholipids are involved in a variety of events such as cellular signalling and trafficking, membrane neogenesis and haemozoin formation. Biogenic amines and amino acids are required by parasites for nucleic acid and protein synthesis (Olszewski et al 2009). We expected that requirements for all these classes of metabolites increases throughout the IDC given the need to metabolise and generate multiple progeny within each parasite. It is unlikely that acylcarnitines are involved in the IDC schedule for two reasons. First, we were unable to find evidence that a lack of acylcarnitines affects the IDC schedule or parasite replication. Second, the acylcarnitines in our screen peaked during fasting when parasites are in their least energetically/metabolically demanding stages. The case for glycerophospholipids is slightly stronger, although the majority of glycerophospholipids in our screen also peaked during host fasting. Glycerophospholipids are needed by the parasite: upon infection, the phospholipid composition of the host RBC changes and there are six times as many phospholipids present in *Plasmodium*-infected RBCs compared to uninfected RBCs (Déchamps et al 2010). During the IDC, parasites scavenge fatty acids and also lysoPCs from the host plasma, which compete with each other as a source of the acyl components required for malarial lipid synthesis. In particular, oleic acid (18:1) increases in the membranes of RBCs during infection (Déchamps et al 2010). We found that lysophosphatidylcholine a C18:1 (lysoPC a 18:1), which contains an oleic acid side chain, is associated with IDC rhythms. However, parasites are able to synthesise these fatty acids de novo via type II FA synthase (FASII) and only require fatty acid synthesis during the liver stage (Tarun et al 2009). Like acylcarnitines, glycerophospholipids peaked during host fasting, and so could only be involved in IDC scheduling if they are used by the parasite for anticipation and do not act as a limiting resource. In contrast, the peaks of amino acids and biogenic amines did coincide with the IDC stages responsible for biogenesis as well as coinciding with the host feeding window. *Plasmodium* must scavenge several amino acids from the host, several of which we found in our screen, including six host-'essential' (isoleucine, leucine, methionine, phenylalanine, threonine and valine) and one host-'non-essential' (alanine) amino acid (Payne and Loomis 2006). Of these, only an exogenous supply of isoleucine is essential for parasites because they can scavenge other amino acids from catabolism of host haemoglobin (Liu et al 2006, Babbitt et al 2012, Martin and Kirk 2007). Isoleucine is the only amino acid absent from human haemoglobin and is one of the least abundant amino acids in rodent haemoglobin (1-3%, Supp Fig 1) yet makes up 9% of both *P. falciparum*'s and *P. chabaudi*'s amino acids (Yadav and Swati 2012). Furthermore, there is no evidence that parasites are able to store isoleucine: the response of *P. falciparum* parasites to isoleucine withdrawal is not influenced by whether they were previously cultured in a high or low isoleucine concentration environment (Babbitt et al 2012). Thus, both hosts and parasites are reliant on the host's food to acquire isoleucine.

Coinciding with the rise in isoleucine concentration during the feeding window, parasites make their transition from trophozoites to schizonts before bursting and beginning development as ring stages at the end of the feeding window (Fig 4). This suggests that the IDC schedule directly follows isoleucine rhythms in the host's blood - put another way, when hosts eat, do their parasites eat as well? That malaria parasites require exogenous isoleucine to complete the IDC is not a new idea. *P. falciparum* parasites *in vitro* are unable to progress the IDC as normal if

bioRxiv preprint doi: https://doi.org/10.1101/2020.08.24.264689; this version posted August 24, 2020. The copyright holder for this preprint (which was not certified by peer review) is the author/funder, who has granted bioRxiv a license to display the preprint in perpetuity. It is made available under aCC-BY 4.0 International license.

isoleucine is missing from their environment (Liu et al 2006, Babbitt et al 2012). When parasites are isoleucine-deprived they undergo delayed cell cycle progression yet are able to recover after a longer period of starvation (~4 IDCs) (Babbitt et al 2012). In contrast, if other amino acids are removed from culture media, parasites switch to scavenging them from haemoglobin with minor effects on the IDC schedule (Babbitt et al 2012). Additionally, not only is isoleucine crucial for the growth of *P. knowlesi* in culture, but parasites only incorporate isoleucine up until the point that schizogony starts (Polet 1968, Polet 1969, Butcher and Cohen 1971, Sherman 1979). Furthermore, isoleucine is one of a few amino acids that are rhythmic in the blood of mice and humans. Specifically, isoleucine was inverted with a 12 h shift in simulated day and night shift work (a phase difference of 11:49 ± 02:10 h between the day and night shift conditions) and follows the timing of food intake (Skene et al 2018).

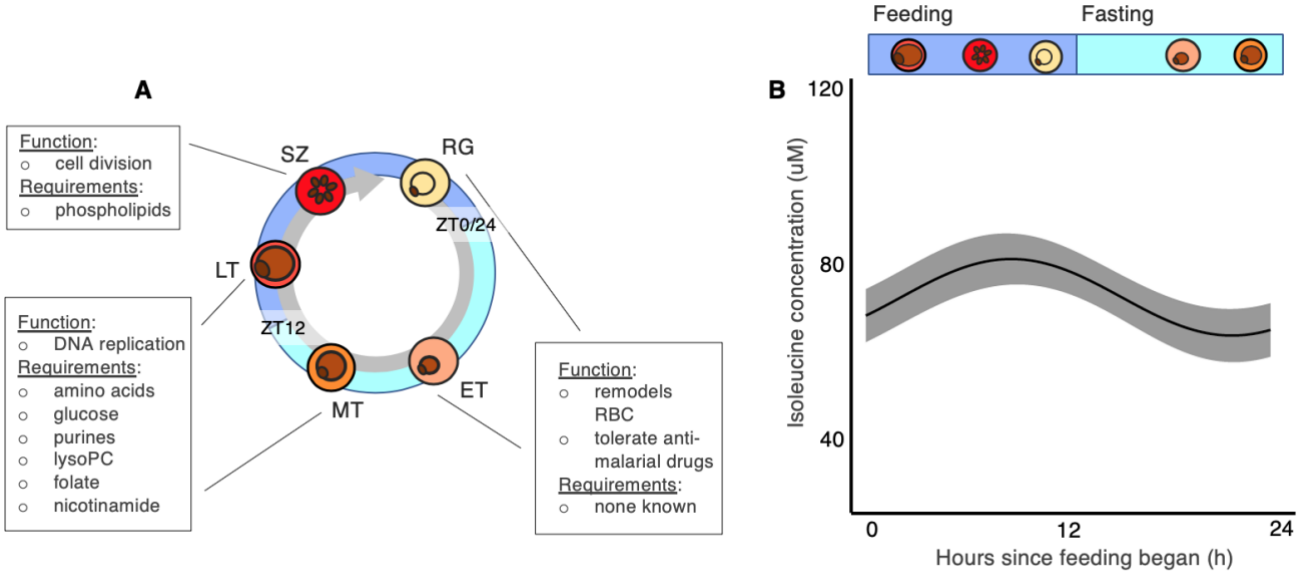

Fig 4. A) The role of each IDC stage in asexual replication and resources known to be essential to each IDC stage. RG=ring stage, ET=early stage trophozoite, MT=mid stage trophozoite, LT=late stage trophozoite, SZ=schizont. B) Model fit (best fit line and 95% prediction interval) for DF, LF and TRF infections combined, of isoleucine concentration in the host blood from the time since feeding commences, with parasite stages overlaid. Stage peaks and intervals taken from Prior et al (2018) and Fig 2. Dark blue bar denotes the 12 h feeding window, light blue bar denotes the 12 h fasting window.

Rhythms in host glucose concentration are not coincident with the IDC schedule

While our screen points to isoleucine being involved in the IDC schedule, previous work implicates blood glucose rhythms (Hirako et al 2018, Prior et al 2018). Specifically, a combination of periodic food intake elevating blood glucose followed by a window of hypoglycaemia each day, caused by immune cell metabolism, are thought to force parasites to undergo energetically demanding IDC completion during the feeding period (Hirako et al 2018). However, unlike for isoleucine, parasites are unable to recover from even just a few hours of glucose starvation (Babbitt et al 2012). Thus, if glucose schedules the IDC it is more likely to do so via enforcing a rhythm (in which mistimed parasites are killed by starvation) than providing information to which the parasite actively modulates its developmental rate. Furthermore, strong immune stimulation – resulting from high parasite densities (the infections examined in Hirako et al 2018 and Prior et al 2018 were ~25% parasitaemia) – may be required to activate sufficient immune cells to generate a high enough amplitude rhythm in blood glucose to schedule the IDC. Such immune stimulation does not occur at the start of infections (Metcalf et al 2011) but rapid rescheduling of the IDC is a highly repeatable phenomenon when infections are initiated with parasites mismatched by 12 hours to the host's rhythm (O'Donnell et al 2011, O'Donnell et al 2013, Prior et al 2018, O'Donnell et al 2019, Subudhi et al 2020). Taken together, these observations suggest that a blood glucose rhythm is not sufficient to explain the IDC schedule. Thus, we test for a role of glucose by examining whether blood-glucose rhythms occur in low parasitaemia infections (~10%) and if the timing of the glucose rhythm coincides with both food intake and the IDC schedule, as they do for isoleucine.

bioRxiv preprint doi: https://doi.org/10.1101/2020.08.24.264689; this version posted August 24, 2020. The copyright holder for this preprint (which was not certified by peer review) is the author/funder, who has granted bioRxiv a license to display the preprint in perpetuity. It is made available under aCC-BY 4.0 International license.

Mean blood-glucose concentration differed between the groups, being higher in DF and TRF mice (DF=8.55±0.14 mmol/L, TRF=8.59±0.13 mmol/L) than in LF and ALF mice (LF=7.90±0.14 mmol/L, ALF=7.68±0.11 mmol/L). We also found that glucose concentration varies throughout the day and that patterns differed between our treatment groups. We used a change in the Akaike Information Criterion for small-sample sizes (AICc) of 2 AICc's (ΔAICc=2) to select the most parsimonious models (Brewer et al 2016). We found two competitive models including only time of day (ZT/h) or both time-of-day and treatment (DF, LF, TRF and ALF) as main effects, that can explain patterns of glucose concentration (Fig 5, Supp Table 6). Specifically, glucose concentration varied throughout the day in DF mice but not much less in LF mice, and glucose did not vary throughout the day in both groups of *Per1/2*-null mice (TRF and ALF) (Supp Table 6). The rhythmic IDC schedule in the DF, LF and TRF groups but the lack of significant rhythmicity in blood glucose in the TRF (and possibly LF) infections suggests something other than glucose ultimately underpins the connection between feeding rhythms and the IDC schedule.

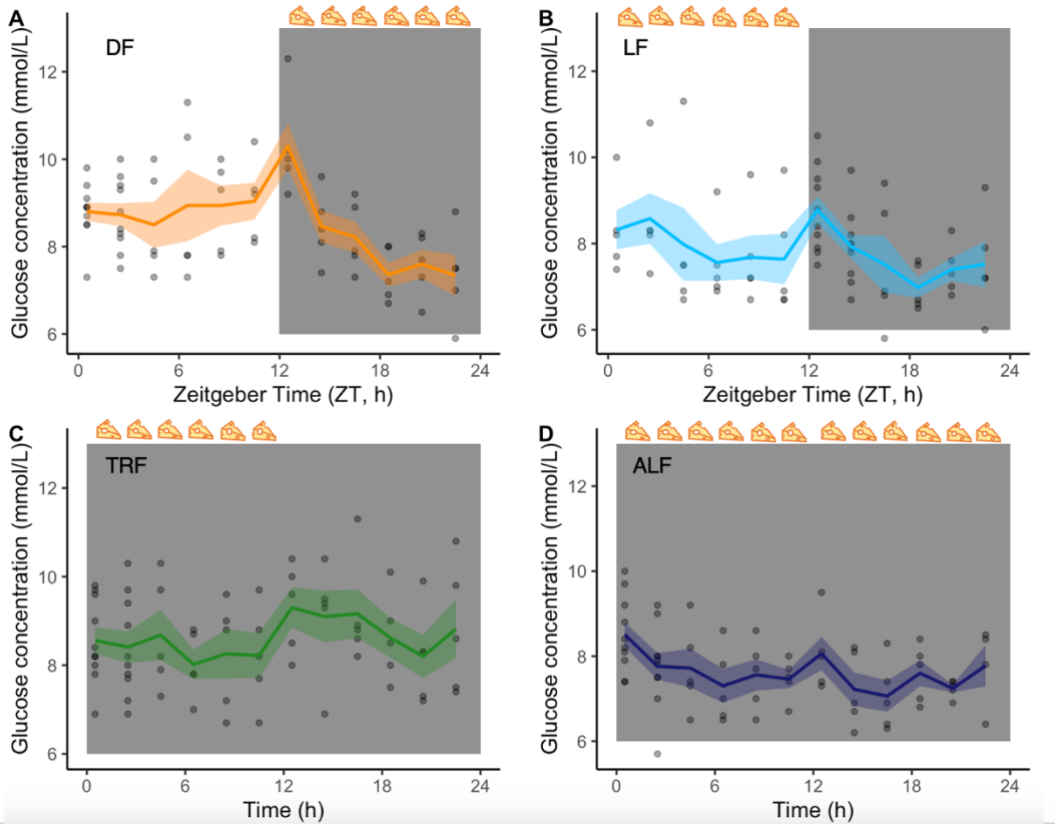

Fig 5. Concentration of glucose (mmol/L) in the blood of A) Wild-type mice with access to food for 12 h at night (ZT 12-24) in 12 h dark:12 h light (DF), B) Wild-type mice with access to food for 12 h in the day (ZT 0-12) in 12h dark:12h light (LF), C) Clock-mutant mice (Per1/2-null) with access to food for the same 12 h as the LF group (0-12 h) in constant darkness (TRF), D) Clock-mutant mice (Per1/2-null) with ad libitum access to food (ALF). The cheeses along the top of plots denotes the feeding windows. The white panel denotes lights on (ZT 0-12 for DF and LF), dark grey panel denotes lights off (ZT 12-24 for DF and LF, 0-24 h for TRF and ALF). The lines and shading are mean ± SEM at each time point and the black dots are the raw data. At time points 0.5 and 2.5 for DF, TRF and ALF, and 12.5 and 14.5 for LF the points are stacked because the time course lasted ~26 hours and the data are plotted on a 0-24 hour axis.

Timing and completion of the parasite IDC depends on the availability of isoleucine

The lack of concordance between the IDC rhythm and variation in blood glucose concentration precludes a direct role for glucose in the IDC schedule, so we next tested if an exogenous supply of isoleucine is capable of scheduling the IDC. We predicted that differences in metabolic requirements across the IDC combined with the daily increase in isoleucine concentration in the blood as a result of host feeding (Fig 4B) keeps the IDC synchronised and timed according to the host feeding rhythm. Due to the difficulty in achieving long term perturbations of isoleucine levels *in vivo* (avoiding off-target confounding effects on the host and interference by host physiology), we used cell culture, following approaches used for *P. falciparum* (Babbitt et al 2012, McLean and Jacobs-Lorena 2020). Specifically, we carried out two experiments in parallel to quantify how *P. chabaudi*'s IDC progression is affected

bioRxiv preprint doi: https://doi.org/10.1101/2020.08.24.264689; this version posted August 24, 2020. The copyright holder for this preprint (which was not certified by peer review) is the author/funder, who has granted bioRxiv a license to display the preprint in perpetuity. It is made available under aCC-BY 4.0 International license.

when isoleucine is removed from media, and whether the IDC is then completed (defined as the proportion of parasites that reach the schizont stage, Supp Fig 2) when isoleucine is returned. First, parasites cultured in the absence of isoleucine (n=32 cultures from the blood of 8 mice, which were split equally across both treatments) develop extremely slowly with approx. 3-fold fewer completing the IDC compared to parasites with isoleucine (50 mg/L, which is the same concentration as RPMI 1640) in their media (n=32 cultures) (Fig 6A). The best fitting model contained only "treatment" (parasites cultured with or without isoleucine) as a main effect (ΔAICc=0, Supp Table 7-A). The reduction in schizonts in isoleucine-free conditions was not due to a higher death rate because the density of parasites remains constant during culture and did not differ between the treatments (Fig 6B) (best fitting model is the null model ΔAICc=0, Supp Table 7-B). Further, incorporating either "treatment" or "hours in culture" into the model did not improve the model fit (treatment: ΔAICc=4.16, hours in culture: ΔAICc=5.50, Supp Table 7-B).

Very slow IDC progression in the absence of isoleucine is consistent with observations of *P. falciparum* (Liu et al 2006, Babbitt et al 2012, McLean and Jacobs-Lorena 2020) and further supported by our second experiment which revealed that development is completed when isoleucine deprivation ends. Parasites (~10^7 per culture) were added to isoleucine-free media and incubated for 7, 14, or 18 hours, after which isoleucine (50 mg/L) was added to their cultures (n=16 cultures per treatment). Parasites completed development when isoleucine became available, regardless of the duration of deprivation (7, 14, or 18 hours), with the best fitting model containing main effects of "treatment" and "hours since isoleucine added" (ΔAICc=0, Supp Table 7-C). Importantly, including the interaction did not improve the model fit (ΔAICc=13.65, Supp Table 7-C), demonstrating that IDC completion proceeds at the same rate despite different durations of isoleucine starvation. Specifically, the rate of IDC completion in the 6-9 hours following isoleucine addition was approximately 50% for all groups (Fig 6C). Again, these completion rates were not driven by higher death rates in cultures deprived of isoleucine for the longest time period because the model incorporating "hours since isoleucine" was competitive with the null model (ΔAICc=0.56, Fig 6D, Supp Table 7-D), revealing parasites were still viable, even after 18 hours in culture (in accordance with Babbitt et al 2012). Furthermore, cultures deprived the longest achieved the most schizonts (18 hours, mean±SEM: 1.61×10^6 ±0.20 Fig 6C), while the fewest schizonts were observed in cultures deprived for the shortest period (7 hours, mean±SEM: 0.83×10^6 ±0.14 Fig 6C). The variation in the intercepts of Fig 6C (<1% schizonts after 7 hours, 3% after 14 hours and 5% after 18 hours deprivation) is likely explained by the 18 hour deprivation cultures accumulating a higher proportion of schizonts at the time of isoleucine provision simply as a product of developing very slowly during a longer window of deprivation. That the absence of isoleucine dramatically slows or stalls development and the provision of isoleucine re-starts development, with negligible consequences for survival is consistent with parasites using isoleucine as a time-of-day cue to synchronise with host rhythms.

bioRxiv preprint doi: https://doi.org/10.1101/2020.08.24.264689; this version posted August 24, 2020. The copyright holder for this preprint (which was not certified by peer review) is the author/funder, who has granted bioRxiv a license to display the preprint in perpetuity. It is made available under aCC-BY 4.0 International license.

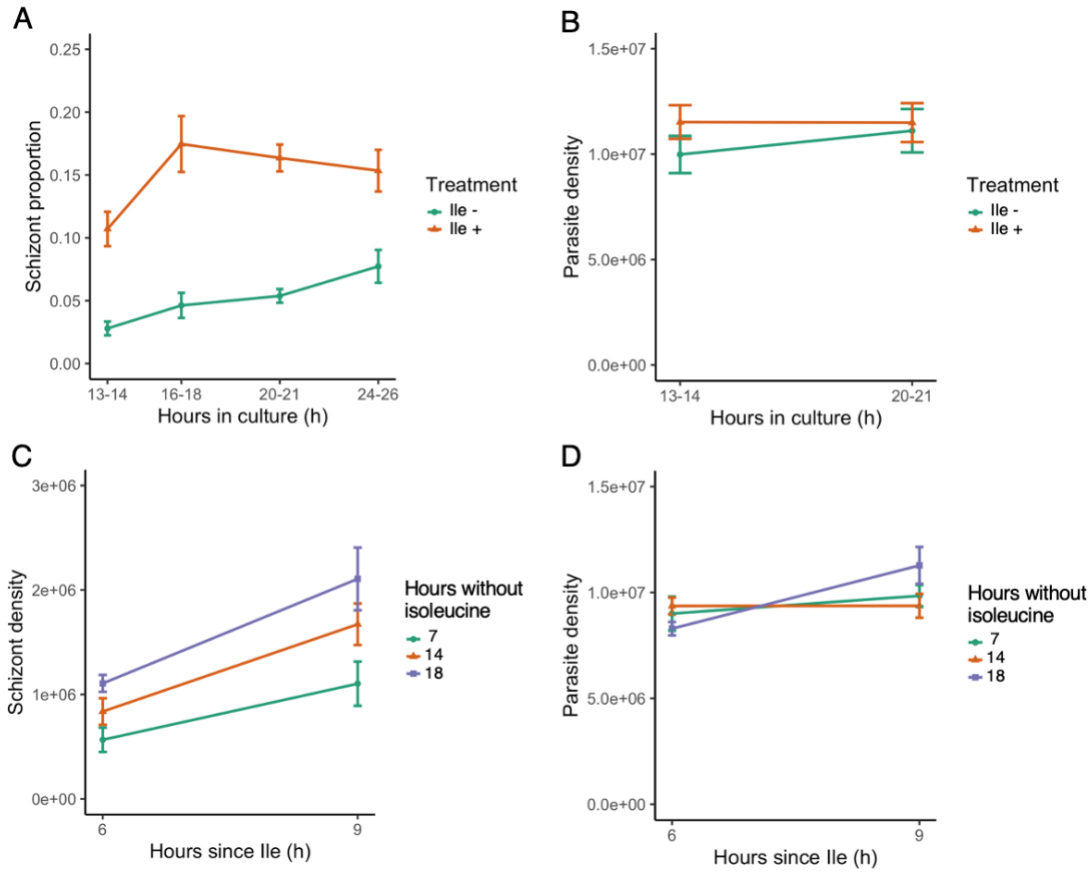

Fig 6. A) IDC completion defined as the proportion of parasites that are schizonts, in cultures with (orange triangles, Ile +, 50 mg/L) or without (green circles, Ile -) isoleucine. B) Density of all parasite stages when parasites are cultured with or without isoleucine. Density C) of schizonts and D) all parasite stages, after the addition of isoleucine into cultures after isoleucine deprivation 7 (green circles), 14 (orange triangles) and 18 hours (purple squares). Proportion of schizonts in the blood seeding the cultures was ~0.005.

Discussion

Why blood-stage malaria parasites exhibit highly synchronised cycles of replication that are timed according to host feeding rhythms is a long-standing question (Prior et al 2020). Our large-scale metabolomics experiment revealed several metabolites that associate with the timing of host feeding, with isoleucine emerging as the best candidate for a role in coordinating the IDC schedule (Fig 3, 4). Further, parasites are sensitive to the presence and absence of isoleucine in their environment, slowing/pausing development when it is absent and then continuing development as normal when isoleucine deprivation ends (Fig 6). Whilst isoleucine is not the only factor essential for IDC completion, and we do not examine vitamins, cofactors, purines and folates which may also be crucial for successful growth (Sherman 1979), our data revealed that isoleucine alone is sufficient to schedule the IDC. Additionally, whilst the lack of rhythmicity in blood glucose concentration in infections with IDC rhythms does not support glucose as a time-cue or scheduling force for the IDC. However, glucose may be indirectly involved. Parasites that are glucose deprived fail to concentrate isoleucine (Martin and Kirk 2007), likely due to a lack of glycolysis and ATP production needed to operate isoleucine transporters (Fig 7). High concentrations of isoleucine in the blood are also associated with uptake of glucose by tissues, potentially contributing to the hypoglycaemia associated with TNF-stimulation of immune cells (Hirako et al 2018). When blood glucose levels are low (e.g. during sickness in rodent models, Elasad and Playfair 1994), parasites are expected to have delayed development due to a lack of time-of-day information and higher mortality due to a lack of resources. In keeping with this, Hirako et al (2018), studying infections with high parasitaemias, found inverted glucose concentration rhythms in light- and dark-fed mice, and that episodes of hypoglycaemia follow schizogony. Additionally, rodent models and humans with obesity and type 2 diabetes like pathologies have elevated levels of isoleucine and dampened glucose rhythms in the blood (Lynch and Adams 2014, Isherwood et al 2017). Thus, if glucose limitation or elevation interferes with the parasite's ability to acquire time-of-day information from isoleucine, the IDC schedule will be disrupted and parasites may desynchronise. In the absence of time-of-day information, even clocks operated by endogenous oscillators desynchronise (Welsh et al 2004, Smith et al 2020). Furthermore, connections between isoleucine and glucose might

bioRxiv preprint doi: https://doi.org/10.1101/2020.08.24.264689; this version posted August 24, 2020. The copyright holder for this preprint (which was not certified by peer review) is the author/funder, who has granted bioRxiv a license to display the preprint in perpetuity. It is made available under aCC-BY 4.0 International license.

explain why the parasite protein kinase 'KIN' is involved in nutrient sensing (Mancio-Silva et al 2017). Identifying KIN (Mancio-Silva et al 2017) and SR10 (Subhudi et al 2020) regulated pathways and determining whether they are sensitive to isoleucine might reveal fundamental components of the parasites' time-keeping mechanism.

Most studies of isoleucine uptake and use in malaria parasites focus on *P. falciparum.* This parasite uses several channels and receptors (both parasite- and host-derived) to acquire resources from the within-host environment (Fig 7A). Uninfected human erythrocytes take up both isoleucine and methionine via the saturable L-system (Cobbold et al 2011), which supplies 20% of the necessary isoleucine (Martin and Kirk 2007). When parasitised, there is a 5-fold increase in isoleucine entering the RBC which is attributable to the presence of new permeability pathways (NPPs) introduced into the RBC membrane by the parasite (Martin and Kirk 2007, McLean and Jacobs-Lorena 2020). NPPs supply 80% of the necessary isoleucine (Martin and Kirk 2007) and are active only in the host membrane at the trophozoite and schizont stages, so it is likely this influx of isoleucine occurs only at certain times of day (e.g. after host feeding, Fig 7B) (Kutner et al 1985). Once inside the RBC, parasitophorous vacuolar membrane (PPM) and parasite plasma membrane (PPM) channels bring nutrients into the parasite, which exchange abundant amino acids that have been released from the digested haemoglobin (such as leucine) for other less abundant amino acids such as isoleucine (Martin and Kirk 2007, Cobbold et al 2011). *P. falciparum* is very sensitive to changes in isoleucine availability; transcription is rapidly slowed upon isoleucine deprivation and isoleucine cannot be stored (Babbitt et al 2012). Assuming *P. chabaudi* has analogous mechanisms, we propose that elevated isoleucine concentration is used by the parasite as a marker for a sufficiently nutrient-rich environment to traverse cell cycle checkpoints and complete the IDC properly (McLean and Jacobs-Lorena 2020, O'Neill et al 2020). For example, parasites might schedule their IDC in response to isoleucine concentration in the blood because it is an essential resource itself and/or because it is a proxy for other essential nutrients that it requires from the host's food (such as folic acid, pantothenic acid, and glucose Müller and Kappes 2007, Müller et al 2010, Hirako et al 2018) that are limiting at certain times of day. Indeed, daily variation in the concentration of isoleucine in the blood appears modest (on average 55 μM to 80 μM from nadir to peak), suggesting that like *P. falciparum, P. chabaudi* is very sensitive to changes in isoleucine levels and that isoleucine is more likely to act on the IDC schedule by providing a time-cue than as a rate limiting resource. Given that the expression of genes associated with translation are the most commonly disrupted when *P. chabaudi*'s rhythms are perturbed (Subhudi et al 2020), we suspect natural selection favours parasites aligning the IDC with the resources required to build proteins.

Scheduling development according to the availability of the resources needed to produce progeny intuitively seems like a good strategy to maximise fitness. Yet, the costs/benefits of the IDC schedule demonstrated by parasites may be mediated by parasite density. At low parasite densities (e.g. at the start of infection), resources may be sufficient to support IDC completion at any time-of-day, but at intermediate densities, parasites may need to align their IDC needs with timing of resource availability. Finally, at very high densities and/or when hosts become sick, resources could be very limiting and a synchronous IDC leads to deleterious competition between related parasites. Quantifying the fitness costs/benefits of using isoleucine to schedule the IDC is even more complicated because coordination with host rhythms impacts asexual replication, transmission stage density, and the infectivity of transmission stages, as well as having downstream consequences for interactions with rhythms experienced within vectors (O'Donnell et al 2011, Pigeault et al 2018, Schneider et al 2018). For example, oocysts in the mosquito come out of dormancy following nutrient replenishment (Habtewold et al 2020): perhaps parasites use isoleucine from the incoming blood meal as a cue to restart development. Furthermore, how isoleucine sensing integrates with a putative endogenous oscillator (Rijo-Ferreira et al 2020, Smith et al 2020) or feeds into a simpler reactionary time keeping strategy (often called a "just-in-time" mechanism) remains to be investigated. SR10 is a likely candidate for modulating IDC duration in response to environmental signals (Subudhi et al 2020) and a parasite stage early in the IDC is likely responsible for time-keeping (McLean and Jacobs-Lorena 2020). The hallmarks of an endogenous oscillator are (i) temperature compensation, (ii) free running in constant conditions, and (iii) entrainment to a Zeitgeber (Pittendrigh 1960). Recent observations are consistent with (ii) (Subudhi et al 2020, Rijo-Ferreira et al 2020, Smith et al 2020) and our results now allow entrainment to isoleucine to be tested for, as well as free-running in isoleucine-constant conditions, to further probe whether malaria parasites possess an endogenous "clock". By understanding how a single metabolite appearing in the blood of the host each day via rhythms in feeding is able to control the timing of parasite replication, it may be possible to improve antimalarial treatments. For example, reducing isoleucine availability without off-target effects on the host may be very difficult, but impairing the parasites ability to detect or respond to isoleucine may stall the IDC, reducing virulence and buy time for host responses to clear the infection.

bioRxiv preprint doi: https://doi.org/10.1101/2020.08.24.264689; this version posted August 24, 2020. The copyright holder for this preprint (which was not certified by peer review) is the author/funder, who has granted bioRxiv a license to display the preprint in perpetuity. It is made available under aCC-BY 4.0 International license.

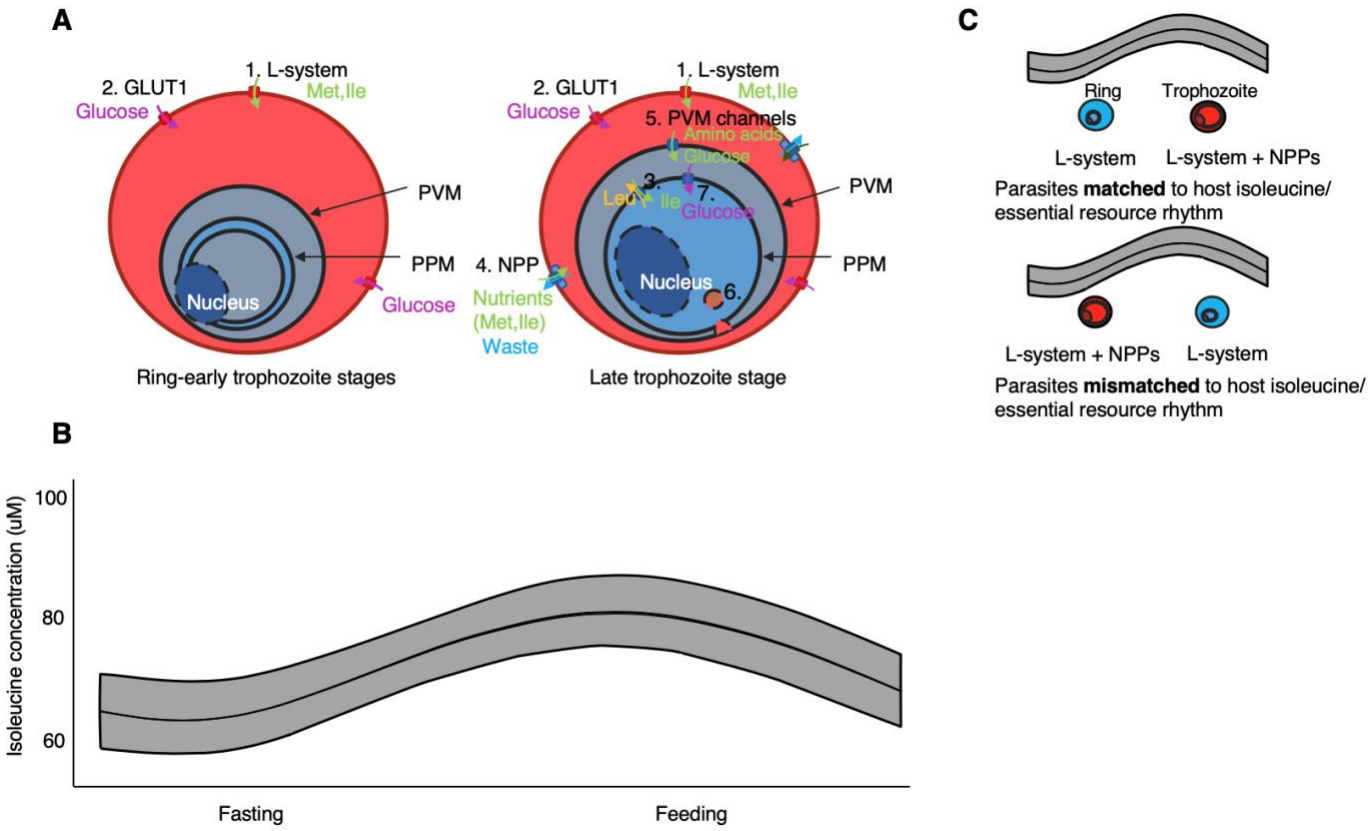

Fig 7. Working model for the connection between the IDC schedule and isoleucine. A) Host and parasite channels/receptors in early and late stage trophozoites, focusing on glucose and isoleucine. 1) Host saturable L-system (Met & Ile) (Cobbold et al 2011), 2) GLUT1, host cell hexose transporter (Landfear 2011), 3) Parasite ATP-independent channels (exchanging leucine for isoleucine until equilibrium is reached), before becoming ATP (glucose)-dependent (Martin and Kirk 2007), 4) Parasite-derived NPPs (New Permeability Pathways, conserved across Plasmodium species, Ngernna 2019) importing nutrients and exporting waste, 5) Parasite-derived PVM channels, 6) Haemoglobin catabolism in parasite lysosome (food vacuole) (Lazarus et al 2008), 7) PfHT1 homologue, parasite hexose transporter, importing glucose to make ATP (Woodrow et al 2000). PVM – parasitophorous vacuolar membrane, PPM – parasite plasma membrane. B) Model fits of the isoleucine rhythm (combined from DF, LF and TRF mice), corresponding to the IDC stages in A to connect the receptors present in the parasite and RBC during host feeding and fasting. C) Illustration of isoleucine concentration in the blood when parasite IDC stages are matched and mismatched to the host feeding rhythm. The NPPs allows acquisition of 80% of necessary isoleucine and the L-system acquires the remaining 20%. Parasites may be affected by isoleucine rhythmicity in two non-mutually exclusive ways: as an essential resource that permits certain IDC stages to exist at certain times of day, and/or as a proxy to indicate the timing of windows when other essential resources are available, enabling maximum exploitation of the host.

Acknowledgements

We thank Daan van der Veen, Sam Rund, Petra Schneider, Alejandra Herbert-Maniero and Ronnie Mooney for practical help and discussion. We also thank the Metabolomics Core Facility at the University of Surrey for doing the LC/MS metabolomics analysis.

Author contributions

KP, AOD, MJB, DS and SR helped design the study. BM, AO, MW and JH helped with the data collection and analysis. All authors contributed to writing the manuscript. KP, AOD and JH are funded by the Wellcome (202769/Z/16/Z). SR is funded by the Wellcome (202769/Z/16/Z) and the Royal Society (UF110155; NF140517). Funding to MJB was from the Francis Crick Institute (https://www.crick.ac.uk/) which receives its core funding from Cancer Research UK (FC001043; https://www.cancerresearchuk.org), the UK Medical Research Council (FC001043;https://www.mrc.ac.uk/), and the Wellcome (FC001043; https://wellcome.ac.uk/). AO is funded by the Wellcome (108905/B/15/Z) and MW by the Darwin Trust (https://darwintrust.bio.ed.ac.uk).

bioRxiv preprint doi: https://doi.org/10.1101/2020.08.24.264689; this version posted August 24, 2020. The copyright holder for this preprint (which was not certified by peer review) is the author/funder, who has granted bioRxiv a license to display the preprint in perpetuity. It is made available under aCC-BY 4.0 International license.

Declaration of Interests

The authors declare no conflicts of interest.

Methods

Blood metabolites

Experimental designs

The same four perturbations of host and parasite rhythms were used in the metabolomics experiment and the glucose monitoring experiment. The *Per1/2*-null mice (non-functional proteins Period 1 & 2, backcrossed onto a C57BL/6 background for over 10 generations) were donated by Michael Hastings (MRC Laboratory of Molecular Biology, Cambridge, UK) and generated by David Weaver (UMass Medical School, Massachusetts, USA). Wild type C57BL/6 mice were housed in a 12h light: 12h dark regime (12 hours of light followed by 12 hours of darkness) and the *Per1/2*-null mice housed in constant darkness (DD) for 2 weeks prior to the start of infections and throughout sampling. We refer to time-of-day using ZT (Zeitgeber Time) for mice housed under entrained conditions (light:dark cycles) and hours when *Per1/2*-null mice are housed under constant conditions (dark:dark). WT mice either had access to food at night (dark feeding, DF) or in the day (light feeding, LF). *Per1/2*-null mice either had access to food for 12 hours (time restricted feeding, TRF) or constant access to food (ad libitum feeding, ALF). Every 12 hours, food was added/removed accordingly from the DF, LF and TRF cages and the cages were checked for evidence of hoarding, which was never observed. ALF cages were also disturbed during food removal/provision of the other groups. We confirmed that parasites in all groups followed the expected synchrony and timing of the IDC, as described in Prior et al (2018) and O'Donnell et al (2019) (Fig 2).

All mice were infected intravenously with ring stage *P. chabaudi* DK genotype with 1×10^5 infected RBC (we deliberately used an avirulent parasite strain, a low parasite dose, and sampled towards the beginning of infection before mice succumbed to infection symptoms, but there were enough parasites to reliably stage the IDC). Sampling started on day 5 post infection and occurred every 2 hours for both the metabolomics and glucose experiments.

All procedures complied with the UK Home Office regulations (Animals Scientific Procedures Act 1986; project licence number 70/8546) and approved by the University of Edinburgh.

Metabolomics experiment

We infected 68 eight-week-old female mice: 35 C57BL/6 wild type animals (DF and LF mice) and 33 *Per1/2*-null TTFL clock-disrupted mice (TRF and ALF) (see Supp Table 2). We sampled mice in blocks (A-D), meaning each individual mouse was sampled every 8 hours during the 26-hour sampling window, with 14 time points in total. We did not sample each mouse at each sampling point to minimise the total volume of blood being taken. At each sampling point for each designated host, 20 µl blood was taken from the tail vein to provide 10 µl blood plasma for snap freezing using dry ice.

Parasite rhythms

We made a thin blood smear each time a mouse was sampled to quantify parasite rhythms by counting ~100 parasites per blood smear using microscopy. Following (Prior et al 2018, O'Donnell et al 2019 and Rijo-Ferreira et al 2020), we used the proportion of ring stages as a phase marker (an estimate of the timing of parasite development in the blood) of parasite rhythms. We calculated amplitude and time-of-day of peak for each treatment group using sine and cosine curves in a linear model to confirm the IDC schedules for each group as used in O'Donnell et al (2019).

Glucose experiment

We infected 20 eight-week-old male mice: 10 C57BL/6 wild type animals and 10 *Per1/2*-null circadian clock-disrupted mice (as described above). We recorded blood glucose concentration from all mice every 2 hours by taking 1 µl blood using an Accu-Chek Performa Nano glucometer (https://www.accu-chek.co.uk/blood-glucose-meters/performa-nano).

bioRxiv preprint doi: https://doi.org/10.1101/2020.08.24.264689; this version posted August 24, 2020. The copyright holder for this preprint (which was not certified by peer review) is the author/funder, who has granted bioRxiv a license to display the preprint in perpetuity. It is made available under aCC-BY 4.0 International license.

Data analysis

Statistical analysis

We identified metabolite candidates by intersecting rhythmic metabolites as determined by circadian programmes (ECHO, CircWave, JTK_Cycle, with period set to 24 hours) and Analysis of Variance in each of our treatment groups (DF, LF and TRF) and excluding those rhythmic in ALF (Fig 2A, Supp Table 1 for numbers of rhythmic metabolites in each group). To calculate the acrophase (timing of peak) we used linear mixed-effects regression models containing sine and cosine terms on all metabolites that varied across the day. Metabolites whose acrophase fell in the same 12h feeding or fasting window (ZT0-12 or ZT12-24) in LF and TRF infections but fell in the opposite window for the DF group were shortlisted as potential connectors between host feeding rhythms and the IDC schedule.

Targeted metabolomics analysis

We quantified metabolites by analysing plasma samples using the AbsoluteIDQ p180 targeted metabolomics kit (Biocrates Life Sciences AG, Innsbruck, Austria) and a Waters Xevo TQ-S mass spectrometer coupled to an Acquity UPLC system (Waters Corporation, Milford, MA, USA) (Isherwood et al 2017, Skene et al 2018). We prepared the plasma samples (10 µl) according to the manufacturer's instructions, adding several stable isotope–labelled standards to the samples prior to the derivatization and extraction steps. Using UPLC/MS (ultra performance liquid chromatography/mass spectrometry), we quantified 185 metabolites from 5 different compound classes (acylcarnitines, amino acids, biogenic amines, glycerophospholipids, and sphingolipids). We ran the samples on two 96-well plates, randomised the sample order and ran three levels of quality control (QC) on each plate. We normalised the data between the plates using the results of quality control level 2 (QC2) repeats across the plate (n=4) and between plates (n=2) using Biocrates METIDQ software (QC2 correction). Metabolites were excluded if the CV% of QC2 was > 30% or if all 4 groups contained > 25% of samples that were below the limit of detection, below the lower limit of quantification, or above the limit of quantification or blank out of range. The remaining 134 quantified metabolites comprised of 7 acylcarnitines, 19 amino acids, 15 biogenic amines, 79 glycerophospholipids and 14 sphingolipids (see Supp Fig 3).

Isoleucine response in culture

Experimental designs

To test the effect of the amino acid isoleucine on the IDC we compared parasite developmental progression in cultures with and without isoleucine (50 mg/L), as well as after different durations (7, 14, 18 hours) of isoleucine starvation. We set up N = 112 cultures (from 8 mice) so that for each time point within each treatment, an independent culture was sampled, avoiding any bias associated with repeat-sampling individual cultures.

Parasites and hosts

We used eight-week-old wild type female mice, MF1 strain, housed in a 12h:12h light:dark regime before and during infection. We infected mice intraperitoneally with 1×10^6 *P. chabaudi* genotype DK infected red blood cells and terminally bled them on day 6 post infection, when the parasitaemia was around 15%. Mice were bled at ZT4, when parasites were late rings/ early trophozoites (see Prior et al 2018). Approximately 1 ml of blood was collected from each mouse which was then split equally across cultures in all 5 treatment groups.

Culturing

We washed infected blood twice with buffered RPMI containing no amino acids (following Spence et al 2011, see Supp Mat "Parasite culture protocol" for more details), before being reconstituted in the RPMI medium corresponding to each treatment (containing isoleucine, or not). We cultured parasites in 96-well round bottom plates with total culture volumes of 200-250 µl, at ~3% haematocrit and kept the culture plates inside a gas chamber which was gassed upon closing with 88% nitrogen 7% carbon dioxide and 5% oxygen, and then placed inside a 37°C incubator. The culture medium was custom made RPMI from Cell Culture Technologies, Switzerland (http://www.cellculture.com) (see Supp Mat "Parasite culture protocol").

Sampling and data

We sampled parasites in the first experiment (comparing IDC completion in isoleucine rich versus isoleucine free media) at 13-14, 16-18, 20-21, 24-26 and 27 hours after culture initiation. We also sampled parasites that had been

bioRxiv preprint doi: https://doi.org/10.1101/2020.08.24.264689; this version posted August 24, 2020. The copyright holder for this preprint (which was not certified by peer review) is the author/funder, who has granted bioRxiv a license to display the preprint in perpetuity. It is made available under aCC-BY 4.0 International license.

isoleucine deprived for 7, 14 or 18 hours at 6 and 9 hrs after isoleucine addition. Samples consisted of a thin blood smear from each culture fixed with methanol and Giemsa stained. We measured the proportion of parasites in the schizont stage (as an indicator of parasites having completed their IDC) by counting ~300 parasites per blood smear. We compared schizont proportion and the density of combined IDC stages using linear regression models.

References

Babbitt, S.E., Altenhofen, L., Cobbold, S.A., Istvan, E.S., Fennell, C., Doerig, C., Llinás, M., and Goldberg, D.E. (2012). *Plasmodium falciparum* responds to amino acid starvation by entering into a hibernatory state. PNAS *109*, E3278-E3287.

Bae, K., Jin, X., Maywood, E.S., Hastings, M.H., Reppert, S.M., and Weaver, D.R. (2001). Differential functions of mPer1, mPer2, and mPer3 in the SCN circadian clock. Neuron *30*, 525-536.

Brewer, M.J., Butler, A., and Cooksley, S.L. (2016). The relative performance of AIC, AICc and BIC in the presence of unobserved heterogeneity. Methods in Ecology and Evolution *7*, 679-692.

Butcher, G.A., and Cohen, S. (1971). Short-term culture of *Plasmodium knowlesi*. Parasitology *62*, 309-320.

Cobbold, S.A., Martin, R.E., and Kirk, K. (2011). Methionine transport in the malaria parasite *Plasmodium falciparum*. Int J Parasitol *41*, 125-135.

Codd, A., Teuscher, F., Kyle, D.E., Cheng, Q., and Gatton, M.L. (2011). Artemisinin-induced parasite dormancy: a plausible mechanism for treatment failure. Malaria Journal *10*, 56. https://doi.org/10.1186/1475-2875-10-56.

Déchamps, S., Shastri, S., Wengelnik, K., and Vial, H.J. (2010). Glycerophospholipid acquisition in *Plasmodium* – a puzzling assembly of biosynthetic pathways. Int J Parasitol *40*, 1347-1365.

Elased, K., and Playfair, J.H.L. (1994). Hypoglycemia and hyperinsulinemia in rodent models of severe malaria infection. Infection and Immunity *62*, 5157-5160.

Garcia, C.R.S., Markus, R.P., and Madeira, L. (2001). Tertian and quartan fevers: temporal regulation in malarial infection. J Biol Rhythms *16*, 436-443.

Grech, K., Watt, K., and Read, A.F. (2006). Host-parasite interactions for virulence and resistance in a malaria model system. J Evol Biol *19*, 1620-1630.

Habtewold, T., Sharma, A.A., Wyer, C.A.S., Masters, E.K.G., Windbichler, N., and Christophides, G.K. (2020). biorXiv, https://doi.org/10.1101/2020.03.07.981951.

Hawking, F. (1970). The clock of the malaria parasite. Scientific American, 123-131.

Hirako, I.C., Assis, P.A., Hojo-Souza, N.S., Reed, G., Nakaya, H., Golenbock, D.T., Coimbra, R.S., and Gazzinelli, R.T. (2018). Daily rhythms of TNF-alpha expression and food intake regulate synchrony of *Plasmodium* stages with the host circadian cycle. Cell Host Microbe *23*, 1-13.

Isherwood, C.M., van der Veen, D.R., Johnston, J.D., and Skene, D.J. (2017). Twenty-four-hour rhythmicity of circulating metabolites: effect of body mass and type 2 diabetes. FASEB J *31*, 5557-5567.

Kutner, S., Breuer, W.V., Ginsburg, H., Aley, S.B., and Cabantchik, Z.I. (1985). Characterization of permeation pathways in the plasma membrane of human erythrocytes infected with early stages of *Plasmodium falciparum*: association with parasite development. Journal of Cellular Physiology *125*, 521-527.

Landfear, S.M. (2011). Nutrient transport and pathogenesis in selected parasitic protozoa. Eukaryot Cell *10*, 483-493.

Lazarus, M.D., Schneider, T.G., and Taraschi, T.F. (2008). A new model for hemoglobin ingestion and transport by the human malaria parasite *Plasmodium falciparum*. J Cell Sci *121*, 1937-1949.

Liu, J., Istvan, E.S., Gluzman, I.Y., Gross, J., and Goldberg, D.E. (2006). *Plasmodium falciparum* ensures its amino acid supply with multiple acquisition pathways and redundant proteolytic enzyme systems. PNAS *103*, 8840-8845.

Lynch, C.J., and Adams, S.H. (2014). Branched-chain amino acids in metabolic signalling and insulin resistance. Nat Rev Endocrinol *10*, 723-736.

bioRxiv preprint doi: https://doi.org/10.1101/2020.08.24.264689; this version posted August 24, 2020. The copyright holder for this preprint (which was not certified by peer review) is the author/funder, who has granted bioRxiv a license to display the preprint in perpetuity. It is made available under aCC-BY 4.0 International license.

Mancio-Silva, L., Slavic, K., Ruivo, M.T.G., Grosso, A.R., Modrzynska, K.K., Vera, I.M., Sales-Diaz, J., Gomes, A.R., MacPherson, C.R., Crozet, P., Adamo, M., Baena-Gonzalez, E., Tewari, R., Llinás, M., Billker, O., and Mota, M.M. (2017). Nutrient sensing modulates malaria parasite virulence. Nature *547*, 213-216.

Martin, R.E., and Kirk, K. (2007). Transport of the essential nutrient isoleucine in human erythrocytes infected with the malaria parasite *Plasmodium falciparum*. Blood *109*, 2217-2224.

Maywood, E.S., Chesham, J., Smyllie, N., Hastings, M. (2014). The Tau mutation of casein kinase 1 sets the period of the mammalian pacemaker via regulation of Period1 or Period2 clock proteins. J Biol Rhythms *29*, 110-118.

McLean, K.J., and Jacobs-Lorena, M. (2020). The response of *Plasmodium falciparum* to isoleucine withdrawal is dependent on the stage of progression through the intraerythrocytic cell cycle. Malar J *19*, 147. doi:10.1186/s12936-020-03220-w

Metcalf, C.J.E., Graham, A.L., Huijben, S., Barclay, V.C., Long, G.H., Grenfell, B.T., Read, A.F., and Bjørnstad, O.N. (2011). Partitioning regulatory mechanisms of within-host malaria dynamics using the effective propagation number. Science *333*, 984-988.

Mideo, N., Reece, S.E., Smith, A.L., and Metcalf, C.J.E. (2013). The Cinderella syndrome: why do malaria-infected cells burst at midnight? Trends Parasitol *29*, 10-16.

Müller, I.B., Hyde, J.E., and Wrenger, C. (2010). Vitamin B metabolism in *Plasmodium falciparum* as a source of drug targets. Trends in Parasitology *26*, 35-43.

Müller, S., and Kappes, B. (2007). Vitamin and cofactor biosynthesis pathways in *Plasmodium* and other apicomplexan parasites. Trends in Parasitology *23*, 112-121.

Ngernna, S., Chim-Ong, A., Roobsoong, W., Sattabongkot, J., Cui, L., and Nguitragool, W. (2019). Efficient synchronization of *Plasmodium knowlesi* in vitro cultures using guanidine hydrochloride. Malar J *18*, 148.

O'Donnell, A.J., Mideo, N., and Reece, S.E. (2013). Disrupting rhythms in *Plasmodium chabaudi*: costs accrue quickly and independently of how infections are initiated. Malar J *12*, 372.

O'Donnell, A.J., Prior, K.F., and Reece, S.E. (2019). Host circadian clocks do not set the schedule for the within-host replication of malaria parasites. biorXiv, https://doi.org/10.1101/777011.

O'Donnell, A.J., Schneider, P., McWatters, H.G., and Reece, S.E. (2011). Fitness costs of disrupting circadian rhythms in malaria parasites. Proc R Soc B *278*, 2429-2436.

O'Neill, J.S., Hoyle, N.P., Robertson, J.B., Edgar, R.S., Beale, A.D., Peak-Chew, S.Y., Day, J., Costa, A.S.H., Frezza, C., and Causton, H.C. (2020). Eukaryotic cell biology is temporally coordinated to support the energetic demands of protein homeostasis. biorXiv, https://doi.org/10.1101/2020.05.14.095521.

Olszewski, K.L., and Llinás, M. (2011). Central carbon metabolism of *Plasmodium* parasites. Molecular & Biochemical Parasitology *175*, 95-103.

Olszewski, K.L., Morrisey, J.M., Wilinski, D., Burns, J.M., Vaidya, A.B., Rabinowitz, J.D., and Llinás, M. (2009). Host-parasite interactions revealed by *Plasmodium falciparum* metabolomics. Cell Host Microbe *5*, 191-199.

Payne, S.H., and Loomis, W.F. (2006). Retention and loss of amino acid biosynthetic pathways based on analysis of whole-genome sequences. Eukaryotic Cell *5*, 272-276.

Pigeault, R., Caudron, Q., Nicot, A., Rivero, A., and Gandon, S. (2018). Timing malaria transmission with mosquito fluctuations. Evolution Letters *2*, 378-389.

Pittendrigh, C.S. (1960). Circadian rhythms and the circadian organization of living systems. Cold Spring Harb Symp Quant Biol *25*, 159-184.

Polet, H., and Conrad, M.E. (1968). Malaria: extracellular amino acid requirements for in vitro growth of erythrocytic forms of *Plasmodium knowlesi*. Proceedings of the Society for Experimental Biology and Medicine *127*, 251-253.

Polet, H., and Conrad, M.E. (1969). The influence of three analogs of isoleucine on in vitro growth and protein synthesis of erythrocytic forms of *Plasmodium knowlesi*. Proceedings of the Society for Experimental Biology and Medicine *130*, 581-586.

bioRxiv preprint doi: https://doi.org/10.1101/2020.08.24.264689; this version posted August 24, 2020. The copyright holder for this preprint (which was not certified by peer review) is the author/funder, who has granted bioRxiv a license to display the preprint in perpetuity. It is made available under aCC-BY 4.0 International license.

649 Prior, K.F., Rijo-Ferreira, F., Assis, P.A., Hirako, I.C., Weaver, D.R., Gazzinelli, R.T., and Reece, S.E. (2020). Periodic
650 parasites and daily host rhythms. Cell Host Microbe *27*, 176-187.

651 Prior, K.F., van der Veen, D.R., O'Donnell, A.J., Cumnock, K., Schneider, D., Pain, A., Subudhi, A., Ramaprasad, A.,
652 Rund, S.S.C., Savill, N.J., and Reece, S.E. (2018). Timing of host feeding drives rhythms in parasite replication. PLoS
653 Pathog *14*, e1006900.

654 Reece, S.E., and Prior, K.F. (2018). Malaria makes the most of mealtimes. Cell Host Microbe *23*, 695-697.

655 Reinke, H., and Asher, G. (2019). Crosstalk between metabolism and circadian clocks. Nature Reviews Molecular Cell
656 Biology *20*, 227-241.

657 Rijo-Ferreira, F., Acosta-Rodriguez, V.A., Abel, J.H., Kornblum, I., Bento, I., Kilaru, G., Klerman, E.B., Mota, M.M., and
658 Takahashi, J.S. (2020). The malaria parasite has an intrinsic clock. Science *368*, 746-753.

659 Schneider, P., Rund, S.S.C., Smith, N.L., Prior, K.F., O'Donnell, A.J., and Reece, S.E. (2018). Adaptive periodicity in the
660 infectivity of malaria gametocytes to mosquitoes. Proc R Soc B *285*, 20181876.

661 Sherman, I.W. (1979). Biochemistry of *Plasmodium* (malarial parasites). Microbiol Rev *43*, 453-495.

662 Skene, D.J., Skornyakov, E., Chowdhury, N.R., Gajula, R.P., Middleton, B., Satterfield, B.C., Porter, K.I., Van Dongen,
663 H.P.A., and Gaddameedhi, S. (2018). Separation of circadian- and behavior-driven metabolite rhythms in humans
664 provides a window on peripheral oscillators and metabolism. PNAS *115*, 7825-7830.

665 Smith, L.M., Motta, F.C., Chopra G., Moch, J.K., Nerem, R.R., Cummins, B., Roche, K.E., Kelliher, C.M., Leman, A.R.,
666 Harer, J., Gedeon, T., Waters, N.C., and Haase, S.B. (2020). An intrinsic oscillator drives the blood stage cycle of the
667 malaria parasite *Plasmodium falciparum*. Science *368*, 754-759.

668 Spence, P.J., Cunningham, D., Jarra, W., Lawton, J., Langhorne, J., and Thompson, J. (2011). Transformation of the
669 rodent malaria parasite *Plasmodium chabaudi*. Nature *6*, 553-561.

670 Subudhi, A.K., O'Donnell, A.J., Ramaprasad, A., Abkallo, H.M., Kaushik, A., Ansari, H.R., Abdel-Haleem, A.M., Rached,
671 F.B., Kaneko, O., Culleton, R., Reece, S.E., and Pain, A. (2020). Malaria parasites regulate intra-erythrocytic
672 development duration via serpentine receptor 10 to coordinate with host rhythms. Nat Commun *11*, 2763.

673 Tarun, A.S., Vaughan, A.M., and Kappe, S.H.I. (2009). Redefining the role of *de novo* fatty acid synthesis in
674 *Plasmodium* parasites. Trends in Parasitology *25*, 545-550.

675 Welsh, D.K., Yoo, S., Liu, A.C., Takahashi, J.S., and Kay, S.A. (2004). Bioluminescence imaging of individual fibroblasts
676 reveals persistent, independently phased circadian rhythms of clock gene expression. Curr Biol *14*, 2289-2295.

677 Woodrow, C.J., Burchmore, R.J., and Krishna, S. (2000). Hexose permeation pathways in *Plasmodium falciparum*-
678 infected erythrocytes. PNAS *97*, 9931-9936.

679 World Malaria Report (2019). https://www.who.int/publications-detail/world-malaria-report-2019

680 Yadav, M.J., and Swati, D. (2012). Comparative genome analysis of six malarial parasites using codon usage bias
681 based tools. Bioinformation *8*, 1230-1239.

682

bioRxiv preprint doi: https://doi.org/10.1101/2020.08.24.264689; this version posted August 24, 2020. The copyright holder for this preprint (which was not certified by peer review) is the author/funder, who has granted bioRxiv a license to display the preprint in perpetuity. It is made available under aCC-BY 4.0 International license.

Supplemental material

Materials and Methods

Parasite culture protocol

Modified from Spence et al (2011).

Equipment

- Water bath (37°C) (Nickel Electro NE3-28DT)
- Heated centrifuge (37°C) (5810R, Eppendorf, Germany)
- Heat block (37°C) (cat. no. N2400-4020, Star Lab, UK)
- Needles and syringes (27 G × 0.5 inch; BD Microlance 3; BD, cat. no. 300635, GP Supplies, UK)
- 15 ml Falcon tubes (cat. no. CLS430055, Sigma-Aldrich, UK)
- Microscope slides (Menzel-Gläser 8037/1, Thermo Scientific, UK)
- Flow cytometer (Z2 Coulter Counter, Beckman Coulter, US)
- Millipore filter (Millex-GP 33 mm PES .22 um Sterile, Merck, US)
- Incubator (37°C) (Panasonic Programmable Cooled Incubator, MIR-154, PHCbi, Japan)
- Cell culture plates (cat. no. SIAL0799, Sigma-Aldrich, UK)
- Compressed gas mixture: 5% O_2, 7% CO_2, 88% N_2 (BOC, UK)
- Incubator chamber

Reagents

- Heparin (cat. no. H3393, Sigma-Aldrich, UK)
- 10% Giemsa's stain (cat. no. 48900-500ML-F, Sigma-Aldrich, UK) in 1× Giemsa's phosphate buffer (cat. no. P4417, Sigma-Aldrich, UK)
- Custom-made RPMI 1640: medium kit "basic RPMI 1640" (without amino acids but including glucose, salts and vitamins) (www.cellculture.com), tissue culture water, sodium hydrogen carbonate.
- Ile- medium: basic RPMI 1640 plus glycine (10 mg/L), L-arginine (200), L-asparagine (50), L-aspartic acid (20), L-cystine 2HCl (65), L-glutamic acid (20), L-glutamine (300 - this is added to the basic RPMI), L-histidine (15), L-hydroxyproline (20), L-leucine (50), L-lysine hydrochloride (40), L-methionine (15), L-phenylalanine (15), L-proline (20), L-serine (30), L-threonine (20), L-tryptophan (5), L-tyrosine disodium salt dihydrate (29)), L-valine (20).
- Ile+ medium: Ile- medium plus L-isoleucine (50 mg/L)
- Buffered RPMI: basic RPMI 1640, 2 µM L-glutamine (cat. no. 25030081, Gibco, UK) and 6 mM HEPES (sterile) (cat. no. 15630080, Gibco, UK).
- Complete RPMI: basic RPMI 1640, 2 mM L-glutamine, 6 mM HEPES, 0.5 mM sodium pyruvate (cat. no. 11360070, Gibco, UK), 50 µM 2-Mercaptoethanol (cat. no. 21985023, Gibco, UK), 10 µl gentamicin (cat. no. 15710049, Gibco, UK), 10% Albumax (sterile) (cat. no. 11021037, Gibco, UK).

Procedure

1. Inject donor mice intraperitoneally with at least 10^6 infected RBC, monitoring the infections daily on Giemsa-stained thin blood films.
2. Around day 6 post infection (or when parasitaemia is around 10-15%), heart bleed mice when parasites are at early trophozoite stage ensuring to use heparin to prevent clotting (around 50-100ul) keeping all equipment at 37°C (tubes, syringes).
3. Collect blood from each mouse into 15 ml Falcon tubes. Measure the total volume of collected blood and for every 1 ml of blood add 10 ml prewarmed buffered RPMI and place in 37°C water bath. Wash blood twice by centrifuging at 2200 rpm/1770 G for 5 mins at 37°C in buffered Ile- medium, split blood between treatment groups, then wash for a second time and resuspend in the correct medium (Ile+ or Ile-).
4. Culture parasites at 2-5% haematocrit ((50×2) × **x** ml blood, assuming hematocrit is 50% in whole blood and **x** is the total amount of blood collected) in Ile+ or Ile- medium, and add 250 ul of the final culture concentration to each well on a 96-well round bottom plate.
5. Stack 96-well plates inside incubator chamber, gas, then place inside 37°C incubator.
6. Sample each well as required using a 10 ul pipette by gently scraping the bottom layer of RBCs and make a thin blood smear. Re-gas the chamber before placing the 96-well plates back in the incubator.

bioRxiv preprint doi: https://doi.org/10.1101/2020.08.24.264689; this version posted August 24, 2020. The copyright holder for this preprint (which was not certified by peer review) is the author/funder, who has granted bioRxiv a license to display the preprint in perpetuity. It is made available under aCC-BY 4.0 International license.

Figures

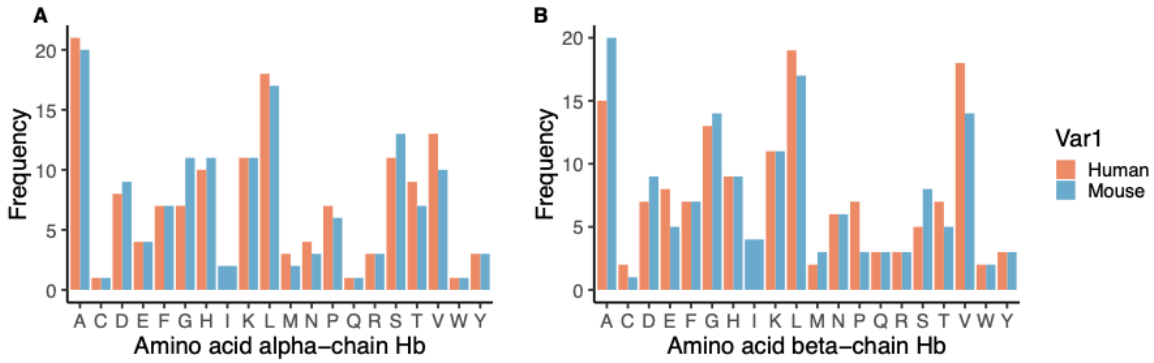

Supp Fig 1. Frequency of amino acids in alpha (A) and beta (B) chains of each human (orange) and mouse (blue) haemoglobin. Amino acid codes: A - alanine, C - cysteine, D - aspartic acid, E - glutamic acid, F - phenylalanine, G - glycine, H - histidine, I - isoleucine, K - lysine, L - leucine, M - methionine, N - asparagine, P - proline, Q - glutamine, R - arginine, S - serine, T - threonine, V - valine, W - tryptophan, Y - tyrosine.

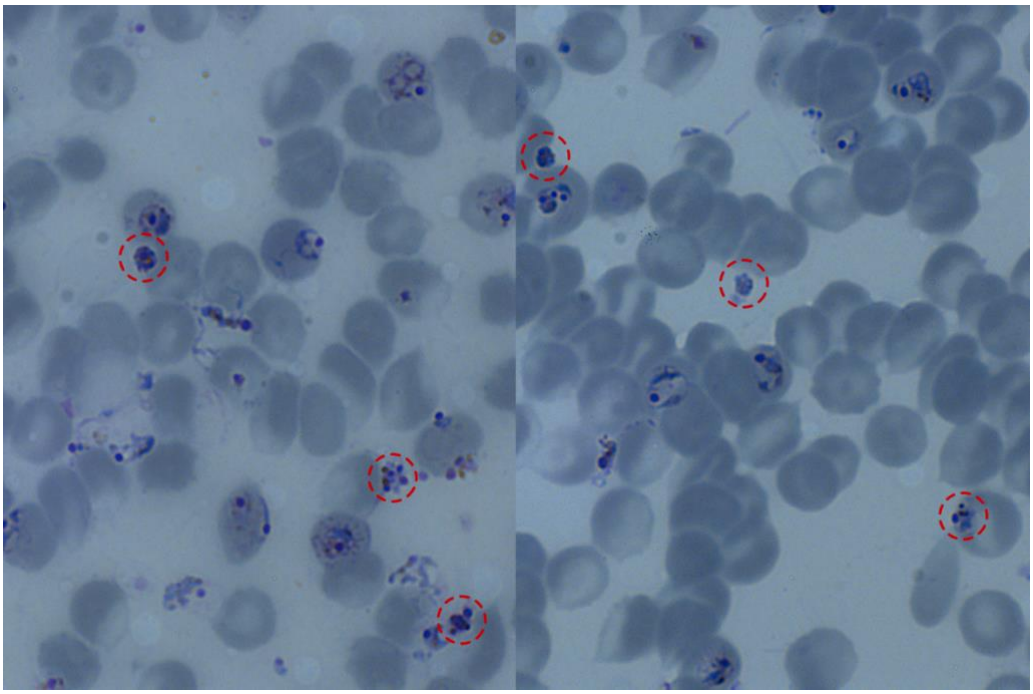

Supp Fig 2. Photo of infected RBCs in P. chabaudi culture, schizonts circled in red. Using Giemsa RBCs stain grey and parasite organelles and nuclei stain blue-purple. Schizonts inside and outside of RBCs were counted (assumed to be viable) as RBC membranes are delicate and are easily disrupted during thin smear production. Parasites spent ~30 h in culture and sampled every 3-4 hours after 13 hours of culture, with each well from the corresponding mouse only being sampled once (n=8 per time point).

bioRxiv preprint doi: https://doi.org/10.1101/2020.08.24.264689; this version posted August 24, 2020. The copyright holder for this preprint (which was not certified by peer review) is the author/funder, who has granted bioRxiv a license to display the preprint in perpetuity. It is made available under aCC-BY 4.0 International license.

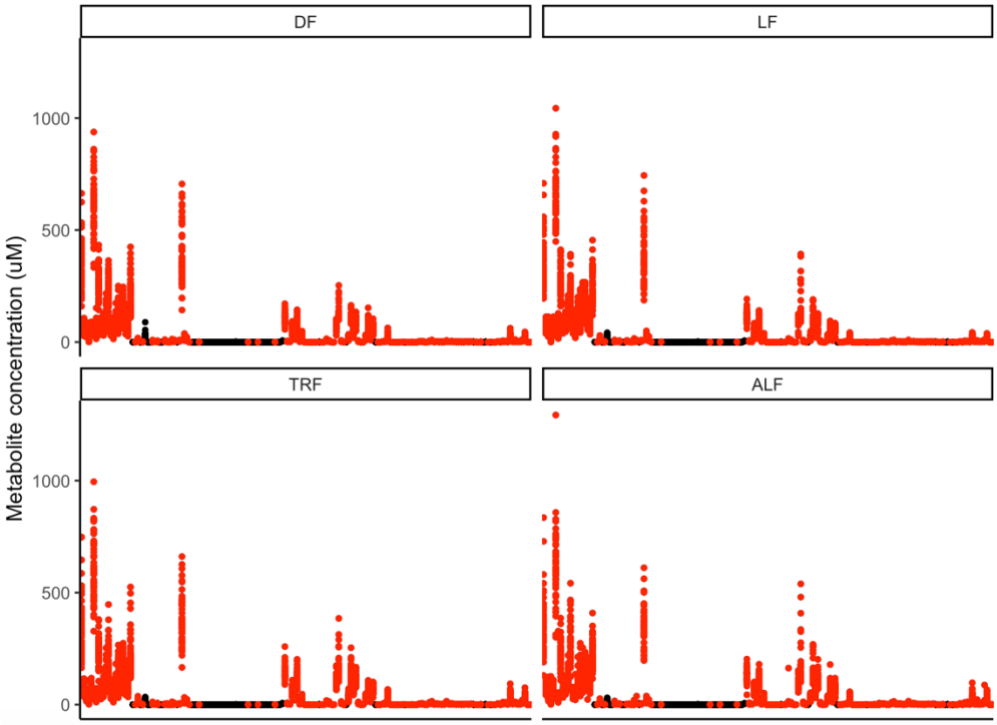

Supp Fig 3. Concentration of all metabolites at all time points during the time series, those included and excluded from the analysis. DF=dark fed wild type mice, LF=light fed wild type mice, TRF=time restricted fed Per1/2-null mice, ALF=ad libitum fed Per1/2-null mice. Each x-axis mark is a different metabolite with concentration (µM) on the y-axis. In black are metabolites excluded since they failed set LC/MS assay criteria and those metabolites taken forward into the analysis are red.

Tables

	Model description: Ring.prop ~	**df**	**logLik**	**AICc**	**ΔAICc**	**AICc *w***
DF	sine + cosine	4	13.30	-16.9	0.00	1.000
	sine	3	-5.77	18.5	35.44	0.000
	cosine	3	-8.69	24.3	41.27	0.000
	null	2	-14.60	33.7	50.60	0.000
LF	sine + cosine	4	8.57	-7.5	0.00	0.788
	sine	3	5.92	-4.9	2.63	0.212
	cosine	3	-1.03	9.0	16.52	0.000
	null	2	-2.68	9.8	17.34	0.000
TRF	sine + cosine	4	21.85	-33.5	0.00	1.000
	sine	3	10.98	-14.7	18.77	0.000
	cosine	3	-0.14	7.5	41.01	0.000
	null	2	-2.54	9.7	43.15	0.000
ALF	sine + cosine	4	32.12	-53.6	0.00	0.995
	sine	3	24.51	-41.5	12.05	0.002
	cosine	3	24.49	-41.5	12.08	0.002
	null	2	19.90	-35.1	18.47	0.000

Supp Table 1. Degrees of Freedom (df), log-Likelihood (logLik), AICc, ΔAICc ($AICc_i - AICc_{min}$) and AICc w (AICc weight) for each linear model in the parasite stage proportion analysis ordered in descending fit (best-fitting model at the top). The response variable for each model is proportion of ring stages (Ring.prop), with "sine" and "cosine" terms being the sine or cosine function of ($2\pi \times$ time of day)/24 with a fixed 24h period fitted for each treatment group (DF, LF, TRF or ALF). AICc is a form of the Akaike Information Criteria corrected for smaller sample sizes to address potential overfitting, used for model selection. Corresponds with Fig 2.

bioRxiv preprint doi: https://doi.org/10.1101/2020.08.24.264689; this version posted August 24, 2020. The copyright holder for this preprint (which was not certified by peer review) is the author/funder, who has granted bioRxiv a license to display the preprint in perpetuity. It is made available under aCC-BY 4.0 International license.

Time (ZT/hours)	0	2	4	6	8	10	12	14	16	18	20	22	24/0	2
A Metabolomics experiment														
Block	*A*	*B*	*C*	*D*	*A*	*B*	*C*	*D*	*A*	*B*	*C*	*D*	*A*	*B*
DF	5	5	4	4	5	5	4	4	5	5	4	4	5	5
LF	5	4	4	4	5	4	4	4	5	4	4	4	5	4
TRF	5	4	4	4	5	4	4	4	5	4	4	4	5	4
ALF	4	4	4	4	4	4	4	4	4	4	4	4	4	4
B Glucose experiment														
DF	5	5	5	5	5	5	5	5	5	5	5	5	5	5
LF	5	5	5	5	5	5	5	5	5	5	5	5	5	5
TRF	5	5	5	5	5	5	5	5	5	5	5	5	5	5
ALF	5	5	5	5	5	5	5	5	5	5	5	5	5	5

Supp Table 2. Mouse numbers for experimental treatment groups. A) Mice in the metabolomics experiment sampled in blocks (A-D) with 4/5 mice per block sampled every 8 hours. Totals for each treatment group: DF=18, LF=17, TRF=17, ALF=16. B) Mice in the glucose experiment were sampled every 2 hours. Totals for each treatment group: DF=5, LF=5, TRF=5, ALF=5. For each experiment repeated measures from mice were controlled for during the analysis.

A

	ECHO		CircWave (CW)		JTK	
	Rhythmic with 24h period	Not-rhythmic with 24h period	Rhythmic with 24h period	Not-rhythmic with 24h period	Rhythmic with 24h period	Not-rhythmic with 24h period
DF	75	59	67	67	47	87
LF	106	28	83	51	70	64
TRF	55	77	41	93	23	111
ALF	2	127	6	128	0	134

B

	ECHO==CW	ECHO==JTK	CW==JTK	Unique
DF	62	47	46	63
LF	79	68	63	88
TRF	37	23	21	39
ALF	1	0	0	1

C

	Not-rhythmic with 24h period	Time-of-day effect	No time-of-day effect	Time-of-day effect + rhythmic with 24h period	Total candidates
DF	71	38	33	101	42
LF	46	3	43	91	
TRF	95	11	84	50	
ALF	133	0	133	1	

bioRxiv preprint doi: https://doi.org/10.1101/2020.08.24.264689; this version posted August 24, 2020. The copyright holder for this preprint (which was not certified by peer review) is the author/funder, who has granted bioRxiv a license to display the preprint in perpetuity. It is made available under aCC-BY 4.0 International license.

Supp Table 3. Metabolite numbers that significantly fluctuate every 24h in the mouse blood for three methods. ***A)*** *Data for all metabolites were run through three circadian programmes to find those following a 24h rhythm using ECHO (Benjamini-Hochberg adjusted p value of 0.05), CircWave (standard p value of 0.05) and JTK_Cycle (BH adjusted p value of 0.05). Metabolites that are excluded using the Surrey LC/MS assay criteria were removed from the analysis (Supp Fig 3).* ***B)*** *Rhythmic metabolites in each programme (ECHO, CircWave and JTK) were intersected, with a metabolite counted as rhythmic if it is significantly rhythmic in at least two programmes (ECHO=CW, ECHO=JTK, CW=JTK).* ***C)*** *The metabolites not fulfilling these criteria were analysed using ANOVA (including time-of-day as a factor), with BH adjusted p values at the 5% level. Metabolites from both methods (circadian programmes and ANOVA) were then combined to perform a final intersection between DF, LF and TRF to find common metabolites. Metabolites rhythmic in ALF mice were then removed.*

Metabolite	Class	DF	LF	TRF	ALF
Ala	Amino.acid				
Arg	Amino.acid				
Asn	Amino.acid				
Asp	Amino.acid				
Cit	Amino.acid				
Gln	Amino.acid				
Glu	Amino.acid				
Gly	Amino.acid				
His	Amino.acid				
Ile	Amino.acid				
Leu	Amino.acid				
Lys	Amino.acid				
Met	Amino.acid				
Orn	Amino.acid				
Phe	Amino.acid				
Pro	Amino.acid				
Ser	Amino.acid				
Thr	Amino.acid				
Trp	Amino.acid				
Tyr	Amino.acid				
Val	Amino.acid				
ADMA	Biogenic_amine				
alpha.AAA	Biogenic_amine				
Carnosine	Biogenic_amine				
Histamine	Biogenic_amine				
Kynurenine	Biogenic_amine				
Met.SO	Biogenic_amine				
Putrescine	Biogenic_amine				
Sarcosine	Biogenic_amine				
SDMA	Biogenic_amine				
Serotonin	Biogenic_amine				
Spermidine	Biogenic_amine				
t4.OH.Pro	Biogenic_amine				
Taurine	Biogenic_amine				
C0	Acylcarnitines				
C2	Acylcarnitines				

bioRxiv preprint doi: https://doi.org/10.1101/2020.08.24.264689; this version posted August 24, 2020. The copyright holder for this preprint (which was not certified by peer review) is the author/funder, who has granted bioRxiv a license to display the preprint in perpetuity. It is made available under aCC-BY 4.0 International license.

C3	Acylcarnitines				
C4	Acylcarnitines				
C14.1	Acylcarnitines				
C16	Acylcarnitines				
C18.1	Acylcarnitines				
lysoPC.a.C16.0	Glycerophospholipids				
lysoPC.a.C16.1	Glycerophospholipids				
lysoPC.a.C17.0	Glycerophospholipids				
lysoPC.a.C18.0	Glycerophospholipids				
lysoPC.a.C18.1	Glycerophospholipids				
lysoPC.a.C18.2	Glycerophospholipids				
lysoPC.a.C20.3	Glycerophospholipids				
lysoPC.a.C20.4	Glycerophospholipids				
lysoPC.a.C24.0	Glycerophospholipids				
lysoPC.a.C26.0	Glycerophospholipids				
lysoPC.a.C26.1	Glycerophospholipids				
lysoPC.a.C28.0	Glycerophospholipids				
lysoPC.a.C28.1	Glycerophospholipids				
PC.aa.C24.0	Glycerophospholipids				
PC.aa.C28.1	Glycerophospholipids				
PC.aa.C30.0	Glycerophospholipids				
PC.aa.C32.0	Glycerophospholipids				
PC.aa.C32.1	Glycerophospholipids				
PC.aa.C32.2	Glycerophospholipids				
PC.aa.C32.3	Glycerophospholipids				
PC.aa.C34.1	Glycerophospholipids				
PC.aa.C34.2	Glycerophospholipids				
PC.aa.C34.3	Glycerophospholipids				
PC.aa.C34.4	Glycerophospholipids				
PC.aa.C36.1	Glycerophospholipids				
PC.aa.C36.2	Glycerophospholipids				
PC.aa.C36.3	Glycerophospholipids				
PC.aa.C36.4	Glycerophospholipids				
PC.aa.C36.5	Glycerophospholipids				
PC.aa.C36.6	Glycerophospholipids				
PC.aa.C38.0	Glycerophospholipids				
PC.aa.C38.3	Glycerophospholipids				
PC.aa.C38.4	Glycerophospholipids				
PC.aa.C38.5	Glycerophospholipids				
PC.aa.C38.6	Glycerophospholipids				
PC.aa.C40.2	Glycerophospholipids				
PC.aa.C40.3	Glycerophospholipids				
PC.aa.C40.4	Glycerophospholipids				
PC.aa.C40.5	Glycerophospholipids				
PC.aa.C40.6	Glycerophospholipids				
PC.aa.C42.0	Glycerophospholipids				
PC.aa.C42.1	Glycerophospholipids				
PC.aa.C42.2	Glycerophospholipids				

bioRxiv preprint doi: https://doi.org/10.1101/2020.08.24.264689; this version posted August 24, 2020. The copyright holder for this preprint (which was not certified by peer review) is the author/funder, who has granted bioRxiv a license to display the preprint in perpetuity. It is made available under aCC-BY 4.0 International license.

PC.aa.C42.4	Glycerophospholipids				
PC.aa.C42.5	Glycerophospholipids				
PC.aa.C42.6	Glycerophospholipids				
PC.ae.C30.1	Glycerophospholipids				
PC.ae.C30.2	Glycerophospholipids				
PC.ae.C32.1	Glycerophospholipids				
PC.ae.C32.2	Glycerophospholipids				
PC.ae.C34.0	Glycerophospholipids				
PC.ae.C34.1	Glycerophospholipids				
PC.ae.C34.2	Glycerophospholipids				
PC.ae.C34.3	Glycerophospholipids				
PC.ae.C36.0	Glycerophospholipids				
PC.ae.C36.1	Glycerophospholipids				
PC.ae.C36.2	Glycerophospholipids				
PC.ae.C36.3	Glycerophospholipids				
PC.ae.C36.4	Glycerophospholipids				
PC.ae.C36.5	Glycerophospholipids				
PC.ae.C38.0	Glycerophospholipids				
PC.ae.C38.1	Glycerophospholipids				
PC.ae.C38.2	Glycerophospholipids				
PC.ae.C38.3	Glycerophospholipids				
PC.ae.C38.4	Glycerophospholipids				
PC.ae.C38.5	Glycerophospholipids				
PC.ae.C38.6	Glycerophospholipids				
PC.ae.C40.1	Glycerophospholipids				
PC.ae.C40.2	Glycerophospholipids				
PC.ae.C40.3	Glycerophospholipids				
PC.ae.C40.4	Glycerophospholipids				
PC.ae.C40.5	Glycerophospholipids				
PC.ae.C40.6	Glycerophospholipids				
PC.ae.C42.1	Glycerophospholipids				
PC.ae.C42.2	Glycerophospholipids				
PC.ae.C42.3	Glycerophospholipids				
PC.ae.C44.3	Glycerophospholipids				
PC.ae.C44.5	Glycerophospholipids				
PC.ae.C44.6	Glycerophospholipids				
SM..OH..C14.1	Sphingolipids				
SM..OH..C16.1	Sphingolipids				
SM..OH..C22.1	Sphingolipids				
SM..OH..C22.2	Sphingolipids				
SM..OH..C24.1	Sphingolipids				
SM.C16.0	Sphingolipids				
SM.C16.1	Sphingolipids				
SM.C18.0	Sphingolipids				
SM.C18.1	Sphingolipids				
SM.C20.2	Sphingolipids				
SM.C24.0	Sphingolipids				
SM.C24.1	Sphingolipids				

bioRxiv preprint doi: https://doi.org/10.1101/2020.08.24.264689; this version posted August 24, 2020. The copyright holder for this preprint (which was not certified by peer review) is the author/funder, who has granted bioRxiv a license to display the preprint in perpetuity. It is made available under aCC-BY 4.0 International license.

SM.C26.0	Sphingolipids				
SM.C26.1	Sphingolipids				

Supp Table 4. Highlighted in green are the metabolites rhythmic in each treatment group (according to the circadian programmes and ANOVA). DF: 101 y, 33 n; LF: 91 y, 43 n; TRF: 50 y, 84 n; ALF: 1 y, 133 n.

Metabolite	Class	DF (ZT, hours)	LF (ZT, hours)	TRF (hours)
C14.1	Acylcarnitines	7.12	20.85	19.13
C16	Acylcarnitines	6.83	19.97	20.44
C18.1	Acylcarnitines	6.65	19.92	20.18
Ala	Amino.acid	19.17	7.99	7.38
Asn	Amino.acid	18.47	6.39	6.03
Asp	Amino.acid	17.46	20.42	18.01
Glu	Amino.acid	17.59	20.08	18.38
Ile	Amino.acid	21.03	7.70	0.40
Leu	Amino.acid	20.36	6.65	2.85
Met	Amino.acid	19.90	6.20	5.90
Phe	Amino.acid	19.78	6.99	5.91
Pro	Amino.acid	19.08	6.95	6.34
Thr	Amino.acid	20.06	7.93	6.33
Val	Amino.acid	20.50	7.95	5.05
ADMA	Biogenic_amine	9.74	20.85	19.43
Carnosine	Biogenic_amine	16.39	20.41	19.03
Histamine	Biogenic_amine	15.27	19.06	19.21
Met.SO	Biogenic_amine	19.37	8.04	6.54
Putrescine	Biogenic_amine	15.80	19.05	16.13
SDMA	Biogenic_amine	9.83	20.78	20.54
Serotonin	Biogenic_amine	13.31	6.29	18.74
Spermidine	Biogenic_amine	16.54	19.78	19.13
Taurine	Biogenic_amine	16.07	20.22	19.60
lysoPCaC16:1	Glycerophospholipids	6.50	18.17	18.20
lysoPCaC18:1	Glycerophospholipids	6.97	18.57	16.64
lysoPCaC18:2	Glycerophospholipids	5.90	15.27	12.05
PCaaC32:1	Glycerophospholipids	1.41	16.26	18.89
PCaaC32:2	Glycerophospholipids	23.87	16.15	18.57
PCaaC34:4	Glycerophospholipids	6.71	17.92	0.54
PCaaC38:3	Glycerophospholipids	7.48	19.01	22.51
PCaaC38:4	Glycerophospholipids	8.18	21.07	1.18
PCaaC38:5	Glycerophospholipids	7.70	20.03	0.89
PCaaC38:6	Glycerophospholipids	6.81	20.36	23.97
PCaaC40:4	Glycerophospholipids	5.80	18.63	23.57
PCaaC40:5	Glycerophospholipids	7.01	19.68	23.88
PCaeC34:1	Glycerophospholipids	23.59	16.45	18.99
PCaeC34:3	Glycerophospholipids	0.48	15.22	14.65
PCaeC36:2	Glycerophospholipids	22.36	12.23	10.04
PCaeC38:0	Glycerophospholipids	7.80	19.97	0.71
PCaeC38:2	Glycerophospholipids	20.45	12.78	9.58

bioRxiv preprint doi: https://doi.org/10.1101/2020.08.24.264689; this version posted August 24, 2020. The copyright holder for this preprint (which was not certified by peer review) is the author/funder, who has granted bioRxiv a license to display the preprint in perpetuity. It is made available under aCC-BY 4.0 International license.

PCaeC38:3	Glycerophospholipids	2.18	16.49	19.91
PCaeC42:1	Glycerophospholipids	8.78	20.70	2.72

Supp Table 5. Timing of peak of each final candidate metabolite in the blood for each treatment group. For LF and TRF groups ZT 0/ 0 hours is the start of the feeding window and the time of lights on for LF, while for DF ZT0 is the start of the fasting window and the time of lights on. LF and DF groups are in 12h:12h light:dark although feeding in the day and night respectively. TRF are in constant darkness although feed for the same 12h window (0-12 hours) as the LF group (same experimenter time). Corresponds with Fig 3B.

	Model description: Glucose.conc ~ + (1|mouseID)	**df**	**logLik**	**AICc**	**ΔAICc**	**AICc *w***
	time	14	-369.71	769.0	0.00	0.555
	treatment + time	17	-366.55	769.4	0.44	0.445
	treatment*time	50	-331.38	785.1	16.12	0.000
	null	3	-390.80	787.7	18.68	0.000
	treatment	6	-387.75	787.8	18.80	0.000
DF	time	14	-90.06	215.7	0.00	0.996
	null	3	-110.28	226.9	11.17	0.004
LF	null	3	-94.83	196.0	0.00	0.550
	time	14	-80.39	196.4	0.40	0.450
TRF	null	3	-85.23	176.8	0.00	0.999
	time	14	-77.54	190.7	13.9	0.001
ALF	null	3	-88.02	182.4	0.00	0.994
	time	14	-78.43	192.6	10.21	0.006

Supp Table 6. Degrees of Freedom (df), log-Likelihood (logLik), AICc, ΔAICc ($AICc_i - AICc_{min}$) and AICc w (AICc weight) for each linear model in the glucose concentration analysis ordered in descending fit (best-fitting model at the top). The response variable for each model is glucose concentration (Glucose.conc) and the random effect is "mouseID". "Treatment" refers to the treatment group (DF, LF, TRF or ALF) and "time" refers to the time-of day (ZT 0-24h or 0-24h) which was fitted as a factor. Corresponds with Fig 5.

Model description:	**df**	**logLik**	**AICc**	**ΔAICc**	**AICc *w***
A) Schizont.prop ~ + (1|mouseID)					
treatment	4	106.26	-203.8	0.00	0.996
treatment + hours in culture	7	104.29	-192.6	11.26	0.004
treatment * hours in culture	10	98.81	-173.5	30.37	0.000
null	3	80.96	-155.5	48.31	0.000
hours in culture	6	74.89	-136.3	67.54	0.000
B) Parasite.dens ~ + (1|mouseID)					
null	3	0.14	6.6	0.00	0.836
treatment	4	-0.63	10.7	4.16	0.104
hours in culture	4	-1.30	12.1	5.50	0.053
treatment + hours in culture	5	-2.07	16.4	9.88	0.006
treatment * hours in culture	6	-2.79	20.9	14.36	0.001
C) Schizont.dens ~ + (1|mouseID)					
treatment + hours since isoleucine	6	69.67	-125.3	0.00	0.887
hours since isoleucine	4	65.04	-121.2	4.14	0.112
treatment * hours since isoleucine	8	65.67	-111.6	13.65	0.001
null	3	56.87	-107.2	18.10	0.000
treatment	5	56.67	-101.9	23.39	0.000

bioRxiv preprint doi: https://doi.org/10.1101/2020.08.24.264689; this version posted August 24, 2020. The copyright holder for this preprint (which was not certified by peer review) is the author/funder, who has granted bioRxiv a license to display the preprint in perpetuity. It is made available under aCC-BY 4.0 International license.

D) Parasite.dens ~ + (1|mouseID)					
hours since isoleucine	4	12.96	-17.0	0.00	0.568
null	3	11.49	-16.4	0.56	0.430
treatment + hours since isoleucine	6	9.10	-4.1	12.85	0.001
treatment	5	7.76	-4.1	12.90	0.001
treatment * hours since isoleucine	8	10.47	-1.2	15.75	0.000

Supp Table 7. Degrees of Freedom (df), log-Likelihood (logLik), AICc, ΔAICc ($AICc_i - AICc_{min}$) and AICc w (AICc weight) for each linear model in the schizont/parasite proportion/density analysis ordered in descending fit (best-fitting model at the top). The response variable for each model is either schizont proportion (Schizont.prop), parasite density (Parasite.dens) or schizont density (Schizont.dens) and the random effect is "mouseID". "Treatment" refers to the treatment group (DF, LF, TRF or ALF), "hours in culture" refers to the number of hours spent in culture since being extracted from the mice, and "hours since isoleucine" refers to the number of hours since isoleucine was added to the cultures. Treatment, hours in culture and hours since isoleucine were all fitted as factors. Corresponds with Fig 6.